TECTONICS, VOL. 20, NO. 3, PAGES 289-307, JUNE 2001

Miocene unroofing of the Canyon Range during extension along the Sevier Desert Detachment, west central Utah

Daniel F. Stockli[1]

Department of Geological and Environmental Sciences, Stanford University, Stanford, California

Jonathan K. Linn[2], J. Douglas Walker

Department of Geology, University of Kansas, Lawrence, Kansas

Trevor A. Dumitru

Department of Geological and Environmental Sciences, Stanford University, Stanford, California

Abstract. Apatite fission track results from Neoproterozoic and Lower Cambrian quartzites collected from the Canyon Range in west central Utah reveal a significant early to middle Miocene cooling event (~19-15 Ma). Preextensional temperatures estimated from multicompositional apatite fission track data suggest ~4.5 to >5.6 km of unroofing during the early to middle Miocene, assuming a geothermal gradient of ~25°C/km. The spatial distribution of these preextensional temperatures indicates ~15°-20° of eastward tilting of the Canyon Range during rapid extensional unroofing along a moderately west dipping detachment fault (~35°-40°). We interpret this fault to be the breakaway of the Sevier Desert Detachment fault (SDD), the existence of which has been contested. The new thermochronologic data presented in this study provide compelling evidence for the existence of the SDD and thus the general viability of low-angle detachment faulting. The data directly date the onset of extensional faulting along the SDD starting at ~19 Ma and constrain the fault slip rate in the SDD breakaway zone at 2.4-2.1 mm/yr between ~19 and 15 Ma. An early Miocene apatite fission track age obtained from a Proterozoic clast from the Tertiary Oak City Formation confirms that these conglomerates were deposited in a synextensional basin in the hanging wall of the SDD. The timing of tectonic unroofing of the Canyon Range in response to faulting along the SDD appears to be synchronous with large-magnitude extension along the Snake Range décollement and with early extension along the Cave Canyon detachment exposed in the Mineral Mountains, pointing to widespread east-west extension in the eastern Great Basin in the early and middle Miocene.

[1]Now at Division of Earth and Planetary Sciences, California Institute of Technology, Pasadena, California.

[2]Now at Eagan McAllister Associates, Inc., Lexington Park, Maryland.

Paper number 2000TC001237.
0278-7407/01/2000TC001237$12.00

1. Introduction

The Canyon Range in west central Utah lies within the Mesozoic Sevier orogenic belt of *Armstrong* [1968] at the eastern margin of the Basin and Range extensional province (Figure 1). The geology of the Canyon Range and the adjacent Sevier Desert region has become the focus of intense scientific debate concerning the regional tectonic evolution of the eastern Great Basin and especially the mechanical and kinematic viability of low-angle detachment faulting in extensional tectonics. Seismic reflection studies in the Sevier Desert basin to the west of the Canyon Range (Figure 1) imaged a prominent ~11°-12° west dipping reflector, the Sevier Desert reflector (SDR). The SDR has been interpreted to represent a top to the west, low-angle extensional fault, the Sevier Desert Detachment (SDD) fault [*McDonald*, 1976; *Wernicke*, 1981; *Wernicke and Burchfiel*, 1982; *Allmendinger et al.*, 1983; *Von Tish et al.*, 1985; *Mitchell and McDonald*, 1987; *Planke and Smith*, 1991]. The magnitude of displacement along the proposed SSD ranges from <10 [*Planke and Smith*, 1991] to 38-45 km [e.g., *Von Tish et al.*, 1985; *Coogan and DeCelles*, 1996; *Mitra and Sussman*, 1997].

The hypothesized SDD has become one of the most famous and classic examples for low-angle detachment faulting challenging models that suggest that low-angle normal faults only slipped at initially higher fault angles [e.g., *Buck*, 1988]. This debate over the mechanical viability of low-angle normal faulting continues, despite recent evidence for seismogenic and active low-angle normal faulting, for example in the D'Entrecasteaux Islands [e.g., *Hill et al.*, 1992; *Abers et al.*, 1997], the Gulf of Corinth [e.g., *Rietbrock et al.*, 1996; *Rigo et al.*, 1996; *Sorel*, 2000], and the central Italian Apennines [e.g., *Boncio et al.*, 2000].

In the past decade the low-angle detachment model for the prominent west dipping reflector below the Sevier Desert and the existence of the SDD has come under serious scrutiny [*Anders and Christie-Blick*, 1994; *Hamilton*, 1994; *Wills and Anders*, 1996; *Wills and Anders*, 1999]. Several workers have contested the existence of the SDD on the basis of lack of deformational fabrics in strata from boreholes near the hypothesized detachment fault [*Anders and Christie-Blick*, 1994] and on aspects of the surface geology near the eastern

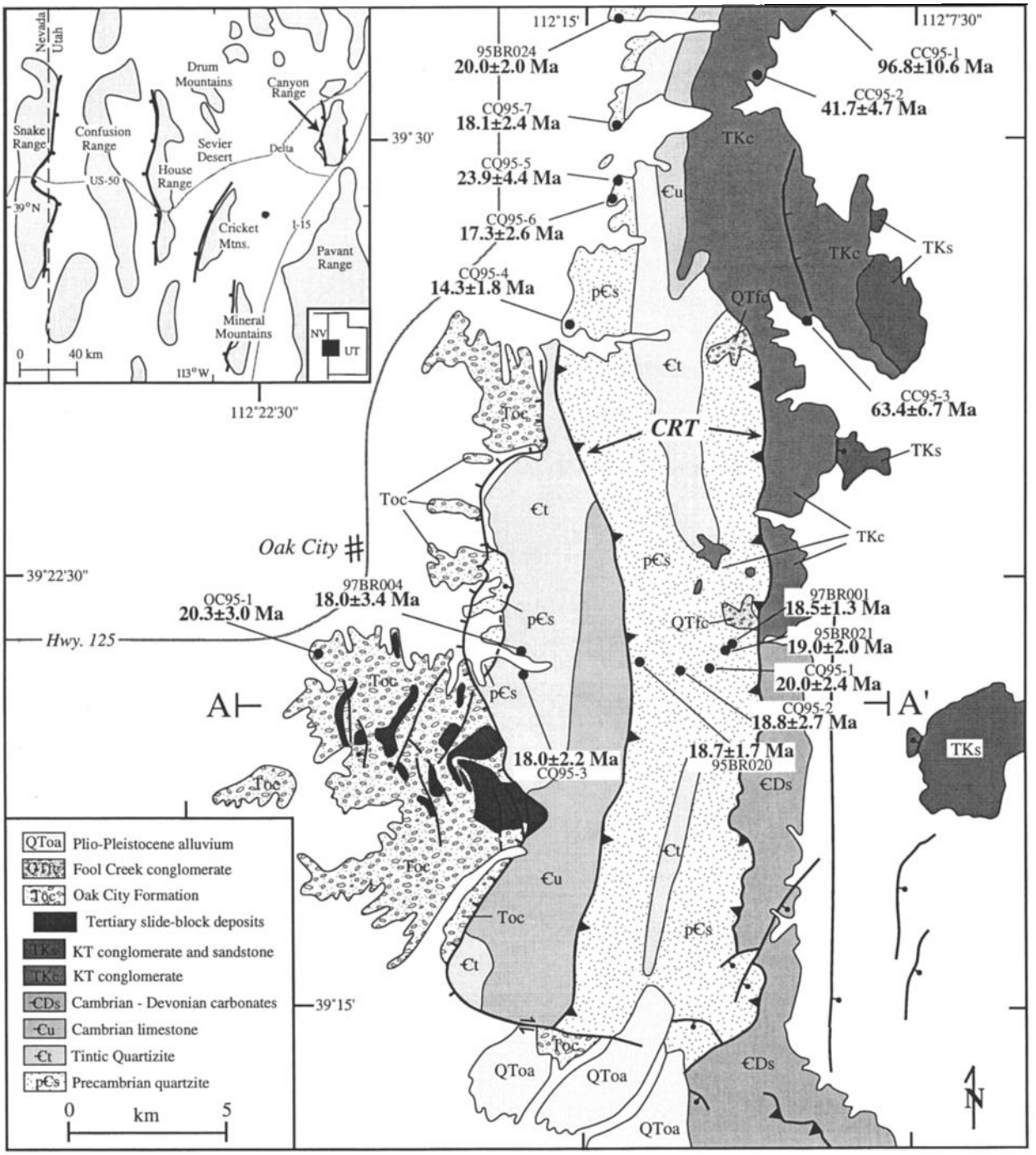

Figure 1. Generalized geologic map of the Canyon Range showing apatite fission track sample localities and results. Unit "Toc" represents rocks in the hanging wall of the proposed Sevier Desert Detachment fault, whereas Proterozoic and Lower Cambrian units are in the footwall. Precambrian quartzites in the hanging wall of the Canyon Range thrust fault (CRT; barbs on upper plate) are indicated by pC. Stratigraphic units: pCs, Precambrian quartzites and minor limestone; Ct, Cambrian Tintic quartzite; Cu, undifferentiated Middle and Upper Cambrian limestone and shale; CDs, Cambrian through Devonian limestone, dolomite, quartzite, and shale; TKc, Cretaceous and Tertiary conglomerate; TKs, Cretaceous and Tertiary conglomerate, sandstone, and shale; Toc, Tertiary Oak City Formation; Tfc, Tertiary Fool Creek conglomerate; Qtoa, Pliocene and Pleistocene alluvium. Pre-Cenozoic geology is modified after *Hintze* [1991a, 1991b, 1991c, 1991d, 1991e, 1991f], and Cenozoic geology is modified after *Otton* [1995].

margin of the Sevier Desert [*Hamilton*, 1994; *Wills and Anders*, 1999]. According to their models, the seismically imaged SDR represents an unconformity between Paleozoic and Tertiary strata along much of its extent, rather than an extensional low-angle detachment fault.

Most tectonic reconstructions of the Sevier Desert region place the surface projection of the SDR and therefore the breakaway of the SDD near or along the western side of the Canyon Range [e.g., *Von Tish et al.*, 1985; *Planke and Smith*, 1991; *Otton*, 1995; *Coogan and DeCelles*, 1996]. Several studies have investigated the surface geology of the Canyon Range in order to shed light on the controversy surrounding the existence of the SDD [*Otton*, 1995; *Morris and Hebertson*, 1996; *Wills and Anders*, 1999]. *Otton* [1995] proposed that the western foothills of the Canyon Range represent the breakaway zone of the extensional detachment system hypothesized to floor the Sevier Desert basin, a view shared by *Coogan and DeCelles* [1996] and *Morris and Hebertson* [1996]. In their model the Tertiary clastic sediments in the western foothills were deposited in a synextensional supradetachment basin above the SDD. This hypothesis has been contested by *Wills and Anders* [1999], who proposed that the Canyon Range is a simple horst block bound by Tertiary high-angle normal faults and that the Tertiary sediments along the western range flank rest unconformably on pre-Mesozoic rocks.

This study presents apatite fission track thermochronological constraints from pre-Mesozoic rocks in the Canyon Range, the first direct radiometric age constraints for the timing of unroofing of the range. These data allow us to critically evaluate these contrasting hypotheses since the different tectonic models predict distinctly different cooling histories for rocks from the Canyon Range. If the range is indeed the breakaway zone of the hypothesized SDD, the derived cooling histories should record exhumation and unroofing related to the onset of rapid fault slip along the SDD [e.g., *Wernicke*, 1985; *Lister and Davis*, 1989]. The resolution of the dispute over whether the SDR is an unconformity or a low-angle detachment fault has important consequences for the ongoing debate on the mechanics and kinematics of low-angle normal faulting. The hypothesized existence of the SDD also has important regional tectonic ramifications, strongly affecting both estimates of total Tertiary extension in the northern Basin and Range province [e.g., *Wernicke*, 1992] as well as thrust geometries and shortening estimates in the Mesozoic Sevier fold and thrust belt [e.g., *Mitra and Sussman*, 1997; *Coogan et al.*, 1995]. Thus understanding the geological significance of the SDR is imperative for the tectonic reconstruction of the eastern Great Basin in Mesozoic and Tertiary times.

2. Geologic Setting

The Canyon Range is one of several north-south trending ranges in the eastern Great Basin that expose stacked thrust sheets of Sevier age containing deformed Neoproterozoic to Mesozoic rocks [*Hintze*, 1980, 1988]. The Canyon Range itself is composed of Neoproterozoic quartzites in the hanging wall and lower Paleozoic sedimentary rocks in the footwall of the Canyon Range thrust fault (CRT) [e.g., *Lawton et al., 1997*]. The CRT is folded into an eastvergent synform by subsequent deformation due to antiformal stacking associated with the underlying Pavant thrust fault (PVT) (Figures 1 and 2) [*Christiansen*, 1952; *Swank*, 1978; *Holladay*, 1984; *Coogan et al.*, 1995; *DeCelles et al.*, 1995; *Mitra and Sussman*, 1997; *Lawton et al.*, 1997]. Contractile deformation purportedly spanned latest Jurassic through Paleocene time and had ceased by Eocene time, as evidenced by the undeformed Eocene Flagstaff Formation [*Armstrong*, 1968; *Villien and Kligfield*, 1986; *Coogan et al.*, 1995; *DeCelles et al.*, 1995]. Initial thrusting along the CRT is constrained by the age of the Cedar Mountain Formation (~130-120 Ma) along the eastern flank of the range, which contains clasts derived from the emerging Canyon Range thrust sheet (Figure

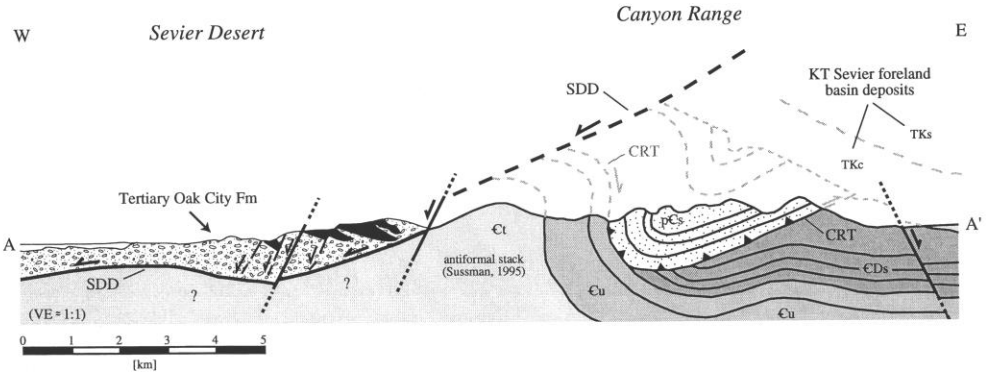

Figure 2. Schematic cross section of the central Canyon Range. Location of cross section is shown on Figure 1. Cross section is modified from *Otton* [1995]. Stratigraphic units: pCs, Precambrian quartzites and minor limestone; Ct, Cambrian Tintic quartzite; Cu, undifferentiated Middle and Upper Cambrian limestone and shale; CDs, Cambrian through Devonian limestone, dolomite, quartzite, and shale; TKc, Cretaceous and Tertiary conglomerate; TKs, Cretaceous and Tertiary conglomerate, sandstone, and shale. Faults: CRT, Canyon Range thrust; SDD, Sevier Desert Detachment.

1) [*DeCelles et al.*, 1995]. Subsequent motion along the PVT in late Aptian to Albian time (~115-98 Ma) resulted in deformation and exhumation of the overlying Canyon Range thrust sheet [*DeCelles et al.*, 1995]. The Canyon Range thrust sheet must have been deeply eroded and subsequently reburied by several kilometers of wedge-top sediments of the Canyon Range Formation during Late Cretaceous to Early Tertiary eastward propagation of thrusting [*Royse*, 1993; *DeCelles et al.*, 1995]. The temporal and spatial succession of contractional deformation documents the overall eastward migration of thrust faulting toward the Sevier foreland with only minor out-of-sequence thrusting [*Lawton et al.*, 1997].

The Canyon Range together with the Pavant Range forms the eastern margin of the Sevier Desert basin. The basin and its origin have attracted substantial interest, with many studies focusing on the nature and origin of the SDR imaged on the Utah-1 line of the COCORP seismic reflection profile and several industrial seismic lines [*Allmendinger et al.*, 1983; *Von Tish et al.*, 1985; *Mitchell and McDonald*, 1987; *Planke and Smith*, 1991; *Coogan and DeCelles*, 1996]. The low-angle reflector dips ~11°-12° to the west and extends from near the western side of the Canyon Range to beneath the Sevier Desert and Cricket Mountains (Figure 1). *Allmendinger et al.* [1983] and *Von Tish et al.* [1985] suggested that the reflector is a down to the west detachment fault, the SDD, with up to 38-45 km of displacement on the basis of offset contractile structures and other geological relationships. *Coogan et al.* [1995] and *Coogan and DeCelles* [1996] argue that major offset along the detachment is required to restore distinctive upper Proterozoic and Cambrian miogeoclinal units in the Cricket Mountains across the Sevier Desert basin to the Canyon Range. Although some controversy exists about the timing of fault slip along the hypothesized SDD, most studies suggest that faulting began after middle Oligocene time (28-26 Ma) and has continued through the Pliocene and might in fact still be active [e.g., *Von Tish et al.*, 1985]. The timing of onset of faulting is constrained by Oligocene lacustrine and volcanoclastic sediments from boreholes in the central Sevier Desert basin that predate extensional faulting [*Lindsey et al.*, 1981; *Mitchell and McDonald*, 1987; *Coogan and DeCelles*, 1996].

The Canyon Range has turned out to be particularly important in the scientific discussion surrounding the nature and tectonic origin of the Sevier Desert basin. The updip projection of the SDR intersecting the surface near the western flank of the range, proposed offsets of Mesozoic contractional structures, and the tilted Tertiary sediments in the western foothills have made the Canyon Range the most likely location for the extensional breakaway of the hypothesized SDD. *Otton* [1995] proposed the presence of an extensional fault zone along the western flank of the Canyon Range, which may represent the breakaway of the SDD (Figure 1), a model contested by *Wills and Anders* [1999]. At the core of these contrasting views are the Tertiary coarse-clastic sediments of the Oak City Formation in the western foothills of the Canyon Range and in particular the age and nature of the basal contact with the pre-Mesozoic basement [*Hintze*, 1991b; *Otton*, 1995; *Morris and Hebertson*, 1996; *Lawton et al.*, 1997; *Wills and Anders*, 1999] (Figures 1 and 2). The sedimentary character and stratigraphic architecture of the Oak City Formation and its large rock avalanche deposits have been discussed in detail by *Otton* [1995], *Morris and Hebertson* [1996], and *Wills and Anders* [1999]. *Otton* [1995] mapped the moderately to steeply east dipping Tertiary conglomerates of the Oak City Formation and proposed a synextensional origin for the deposits related to detachment faulting along the SDD. He also presented evidence for a low-angle normal fault contact that dips 18°-24° to the west, juxtaposing synextensional, east tilted Tertiary conglomerates and Neoproterozoic and Cambrian strata in the breakaway zone (Figure 2). In contrast, *Wills and Anders* [1999] claimed that the Oak City Formation rests unconformably on pre-Mesozoic rocks. However, owing to the weathering characteristics of the Tertiary conglomerates the basal contact of the Oak City Formation is largely obscured and covered by colluvium.

Further complicating the understanding of the depositional nature of the Oak City Formation and its regional tectonic implications is the general lack of reliable age constraints. Age assignments are primarily derived from tentative regional correlations and intuition. A Miocene-Pliocene age was proposed for the Oak City Formation by *Campbell* [1979] on the basis of general views on the age of Basin and Range extension at the time. *Otton* [1995] assigned a tentative Miocene age to the Oak City Formation primarily on the basis of a 12.4±1.4 Ma zircon fission track age for a tuff within an Oak City Formation equivalent in the northern Pavant Range (Figure 1). *Wills and Anders* [1999], however, pointed out that even this age is questionable since the tuff is not actually interbedded with these conglomerates but only covered by alluvium derived from them. This observation implies that most of the conglomerates of the Oak City Formation are older than ~12 Ma, if they are indeed correlative with the deposits to the west of the Pavant Range.

The east side of the modern Canyon Range appears to be controlled by an active high-angle normal fault [*Christiansen*, 1952; *Campbell*, 1979; *Millard*, 1983; *Holladay*, 1984; *Hintze*, 1991f; *Wills and Anders*, 1999]. *Millard* [1983] identified a normal fault with up to 450 m offset near the range front, and *Holladay* [1984] suggested a connection between the range-bounding fault and an east side down normal fault identified within the Late Cretaceous–early Tertiary Canyon Range Formation with ~1.2 km of throw. Along the western range front, geomorphic features indicate active uplift along a west dipping, high-angle normal fault that juxtaposes Neoproterozoic Pocatello Formation and Tintic quartzite [*Sussman*, 1995; *Wills and Anders*, 1999]. Offset along this western range-bounding normal fault was estimated at ~1.25 km [*Wills and Anders*, 1999] (Figures 1 and 2). However, *Otton* [1995] interpreted the same fault as an early Tertiary normal fault, and *Holladay* [1984] originally mapped the contact as a Mesozoic thrust fault. Nevertheless, these range-bounding faults led *Wills and Anders* [1999] to propose a tectonic model envisaging the uplift and exhumation of the Canyon Range entirely as a simple horst block bound by high-angle normal faults on the western and eastern flanks of the range.

3. Apatite Fission Track Thermochronology

Apatite fission tracks are linear damage trails in the crystal lattice that form as the result of spontaneous nuclear fission of

trace ^{238}U nuclei [*Fleischer* et al., 1975; *Wagner and Van den haute*, 1992]. Use of apatite fission track data for reconstructing cooling and unroofing histories relies on the fact that new ^{238}U fission tracks form at an essentially constant rate and with an essentially constant initial track length, while older tracks are simultaneously annealed (and ultimately erased) at elevated subsurface temperatures [*Gleadow et al.*, 1986; *Green et al.*, 1989b; *Dumitru*, 2000]. The annealing process causes easily measured reductions in both track lengths and fission track ages [*Naeser*, 1981; *Gleadow et al.*, 1986; *Green et al.*, 1989a, 1989b; *Corrigan*, 1993]. At temperatures hotter than ~110°-150°C, all fission tracks are totally annealed, resetting the fission track clock to zero. Tracks are partially annealed between ~60° and ~110°C, a temperature range termed the partial annealing zone (PAZ). Below ~60°C, fission tracks in apatite are effectively stable, and annealing occurs only at very slow rates [e.g., *Gleadow et al.*, 1986; *Vrolijk et al.*, 1992].

Apatite fission track thermochronology is an effective tool for directly dating the exhumation and cooling of footwall rocks in response to extensional faulting and many studies have successfully utilized this approach to investigate the low-temperature cooling histories of exhumed footwall rocks in the Basin and Range province [*Foster et al.*, 1990; *Fitzgerald et al.*, 1991; *Gans et al.*, 1991; *Howard and Foster*, 1996; *Miller et al.*, 1999; *Stockli et al.*, 2000]. In this study, the technique is employed to constrain the exhumation history of the Canyon Range and to evaluate the implications of the cooling history of the presumed footwall of the SDD for the regional tectonic evolution.

3.1. Apatite Compositional Variations

The annealing rate of fission tracks and the temperature at which all tracks are totally annealed can be correlated with apatite chemistry, principally Cl content [*Green et al.*, 1985, 1986, 1989b], or etching characteristics using the mean etch pit diameter parallel to the crystallographic c axis (parameter D_{par}) [*Burtner et al.*, 1994; *Carlson et al.*, 1999]. Estimates of the total annealing temperature of relatively chlorine-rich, large Dpar apatites range from ~110° to 150°C [*Green et al.*, 1989b; *Corrigan*, 1993; *Ketcham et al.*, 1999], whereas relatively fluorine-rich, small D_{par} apatites are completely annealed above temperatures of ~90°-110°C [*Laslett et al.*, 1987; *Green et al.*, 1989b; *Carlson et al.*, 1999; *Ketcham et al.*, 1999]. Accounting for this range of kinetic behaviors is important for the analysis of samples containing apatite grains spanning a range of Cl and/or D_{par} values. In particular, if such rocks undergo a protracted cooling history, large D_{par}, Cl-apatites yield older fission track apparent ages and exhibit a different track length distribution than small D_{par}, (F, Cl, OH)-apatites even though they experienced identical thermal histories. Thus calculating an apparent apatite fission track age or track length distribution of a sample without determining the compositional variations within the sample may lead to erroneous interpretations. This is particularly critical in sedimentary rocks that commonly contain detrital apatite derived from several provenance regions.

In this study, the etch figure method of *Donelick* [1993; see also *Burtner et al.*, 1994; *Carlson et al.*, 1999] was used to assess the annealing kinetic variations of individual apatite grains. Etch figures are the cross sections of fission tracks that form at the polished and etched surface of apatite grains. The size of these figures is in part a function of the bulk etch rate of the particular apatite grain. The bulk etch rate is a function of apatite composition, with higher-Cl grains generally etching faster than end-member (F, Cl, OH)-apatite. Etch figure data are collected by measuring and averaging the maximum dimensions of etch figures of three or four near-vertical fission tracks in each apatite grain. Absolute D_{par} values depend upon etching conditions; etching with 5.5 *N* HNO_3 for 20 s at 21°-22°C places the boundary between large D_{par}, Cl-apatite and small D_{par}, (F, Cl, OH)-apatite at a D_{par} value of ~2.0 μm [*Donelick et al.*, 1999]. In this study, we etched CQ, CO, and CC samples using 5.5 *N* HNO_3 for 20 s at 22°C, identical to the conditions of *Donelick et al.* [1999]. All BR samples were etched using 5.0 *N* HNO_3 for 20 s at room temperature (20°-23°C) (Table 1).

Track length distributions are also affected by kinetic variations since track lengths in Cl-apatite grains are reduced at higher temperatures. If Cl-apatite grains were partially annealed prior to exhumation, they would be characterized by shorter mean track lengths, reducing the overall mean length of the total population. However, both etch figure size and track lengths are a function of bulk etch rate, which implies that large etch figure lengths in Cl-apatite correspond to slightly longer initial track lengths [see *Burtner et al.*, 1994, Appendix 2; *Carlson et al.*, 1999]. Therefore rapidly cooled Cl-apatite grains, such as from volcanic samples, are characterized by slightly longer mean track lengths than (F, Cl, OH)-apatites from the same sample. This is also suggested by the fact that track lengths and etch figure values in the commonly used Fish Canyon Tuff apatite standard are larger than those in Durango apatite, which has a lower Cl content [*Carlson et al.*, 1999].

3.2. Fission Track Analysis Results

A total of 16 samples (~20-30 kg) were collected and analyzed from the western front of the Canyon Range, from an east-west transect across the central part of the range along Oak Creek, and from Cretaceous synorogenic conglomerates from the northeastern flank of the range (Figures 1 and 2). Twelve of the samples are quartzites from the Neoproterozoic Pocatello Formation and the Lower Cambrian Tintic quartzite. Apatite yields from these units were commonly very small. In particular, the compositionally mature Tintic quartzite contains little to no apatite. An additional 10 samples were collected but could not be analyzed owing to insufficient apatite yields. One sample was collected from conglomerates in the lower part of the Miocene Oak City Formation. Apatite fission track ages and mean confined track length data from all samples analyzed are presented in Table 1. Apatite fission track data presented in this study were initially collected as part of two independent studies using slightly different analytical parameters (Table 1). Specifically, etching conditions vary, slightly affecting the etch figure technique which was employed to estimate variability of apatite annealing kinetics.

The averaging effect of lumping multikinetic or multicompositional age and length populations may obscure the thermal history information recorded by a sample. Apparent apatite fission track ages are plotted against etch figure lengths for six selected samples (Figure 3), which were

Table 1. Apatite Fission Track Data from the Canyon Range, Utah[a]

Sample	Lat./Long., degree	Unit	Elev., m	number Xls	ρ_d	N_d	ρ_s	N_s	ρ_i	N_i	AFT age, Ma ± 1σ	$P(X^2)$	Mean FT Length, μm ± 1σ (*n*)	Mean FT Length ^{252}Cf, μm ± 1σ (*n*)
CQ95-1	39°21'20"/112°13'04"	Mutual Formation	2160	28	1.598	5982	0.561	285	7.805	3965	20.0±2.4	10.0	13.27±1.42 (4)	13.81±0.15 (81)
CQ95-2	39°21'18"/112°12'02"	Mutual Formation	2080	25	1.598	5982	0.335	128	4.967	1897	18.8±2.7	63.0	13.97±0.12 (3)	13.94±0.24 (21)
CQ95-3	39°20'54"/112°15'49"	Tintic Quartzite	1920	24	1.560	5841	0.464	213	6.998	3210	18.0±2.2	11.0	13.90±1.46 (6)	13.66±0.13 (87)
CQ95-4	39°26'44"/112°15'41"	Mutual Formation	1680	36	1.567	5866	0.363	210	6.942	4012	14.3±1.8	46.0	14.13±1.12 (7)	13.70±0.19 (44)
CQ95-5	39°29'28"/112°14'33"	Mutual Formation	1560	11	1.560	5841	0.237	48	2.687	545	23.9±4.4	81.0	12.56±0.96 (2)	n/a
CQ95-6	39°28'49"/112°14'35"	Mutual Formation	1600	10	1.598	5982	0.309	91	4.963	1462	17.3±2.6	1.0	— (0)	13.28±0.31 (30)
CQ95-7	39°29'56"/112°14'05"	Mutual Formation	1600	15	1.560	5841	0.522	146	7.822	2187	18.1±2.4	100.0	14.06±0.81 (10)	13.70±0.25 (44)
95BR020	39°21'23"/112°11'44"	Mutual Formation	1792	20	1.984	5455	0.345	94	4.834	1357	18.7±1.7	79.0	13.74±0.22 (23)	n/a
95BR021	39°21'30"/112°13'46"	Mutual Formation	2006	14	1.977	5455	0.255	28	4.276	594	19.0 ± 2.0	67.0	13.96±1.11 (3)	n/a
95BR024	39°29'55"/112°14'25"	Mutual Formation	1576	10	1.977	5455	0.332	72	4.937	883	20.0 ± 2.0	33.0	13.73±0.25 (8)	n/a
97BR001	39°21'24"/112°11'42"	Mutual Formation	2250	20	1.586	4665	0.233	255	3.538	3574	18.5±1.3	99.0	14.21±0.32 (20)	n/a
97BR004	39°21'12"/112°15'48"	Tintic Quartzite	1830	8	1.603	4665	0.236	30	3.738	476	18.0±3.4	86.0	— (0)	n/a
OC95-1	39°21'13"/112°21'14"	Oak City Formation	1600	11	1.560	5841	0.485	95	6.450	1264	20.3±3.0	96.0	— (0)	n/a
CC95-1	39°32'27"/112°04'57"	Cret. conglomerate	1560	40	1.560	5841	5.658	775	15.922	2214	96.8±10.6	12.0	12.16±1.73 (20)	n/a
CC95-2	39°31'21"/112°04'00"	Cret. conglomerate	1850	41	1.560	5841	2.888	532	18.641	3526	41.7±4.7	0.8	13.18±2.47 (19)	n/a
CC95-3	39°26'40"/112°09'13"	Cret. conglomerate	1780	37	1.560	5841	4.850	1087	20.239	4638	63.4±6.7	0.2	12.07±1.77 (20)	n/a

[a]Abbreviations are Lat., latitude; Long., longitude; Elev., sample elevation; number Xls, number of individual grains dated; ρ_d, induced track density in external detector adjacent to dosimetry glass (x 10^6 tracks per square centimeter); N_d, number of tracks counted in determining ρ_d; ρ_s, spontaneous track density (x 10^6 tracks per square centimeter); N_s, number of spontaneous tracks counted; ρ_i, induced track density in external detector (muscovite) (x 10^6 tracks per square centimeter); N_i, number of induced tracks counted; $P(X^2)$, X^2 probability [*Galbraith*, 1981; *Green*, 1981]; Cret., Cretaceous; n/a, not applicable; Age is the sample central fission track age [*Galbraith and Laslett*, 1993] calculated using the zeta calibration method [*Hurford and Green*, 1983]. The following is a summary of key laboratory procedures. Samples were analyzed by J. Linn (CQ, OC, CC; zeta calibration factor of 349±4) and D. Stockli (BR and ^{252}Cf; zeta factor of 356±5). Apatites were etched for 20 s in 5 *N* (BR) and 5.5 *N* (CQ, CO, and CC) nitric acid at room temperature (20°-23°C). Grains were dated by external detector method with muscovite detectors. The CN5 dosimetry glass was used as a neutron flux monitor. Samples were irradiated in well thermalized positions at Texas A&M (CQ,OC,and CC) and Oregon State University (BR) TRIGA reactor. External detectors were etched in 48% HF. Tracks (BR) were counted with Zeiss Axioskop microscope with 100 times air objective, 1.25 times tube factor, 10 times eyepieces, transmitted light with supplementary reflected light as needed; external detector prints were located with Kinetek automated scanning stage [*Dumitru*, 1993]. Samples (CQ, CO, and CQ) were counted using analytical procedures of *Corrigan* [1993]. Only grains with *c* axes subparallel to slide plane were dated. Confined tracks lengths were measured only in grains with *c* axes subparallel to slide plane; only horizontal tracks measured (within ±5°-10°), following protocols of *Laslett et al.* [1982]. Lengths were measured with computer digitizing tablet and drawing tube, calibrated against stage micrometer [e.g., *Dumitru*, 1993]. Data reduction was done with program (MacTrax) by R. Brown. Modeling done with Monte Trax of *Gallagher* [1995]. Summary of thermal history modeling parameters used (1) binned track lengths data and central fission track age, (2) ±10% uncertainty on observed age, (3) ±0.35 μm uncertainty on mean track length, (4) ±0.5 μm uncertainty on standard deviation of track length distribution, (5) initial track length of 16.3 μm, (6) Durango apatite annealing model of *Laslett at al.* [1987], (7) generic algorithm method modeling with 200 runs and 40 iterations, and (8) output plots showing runs that pass both length and age data at 95% confidence level.

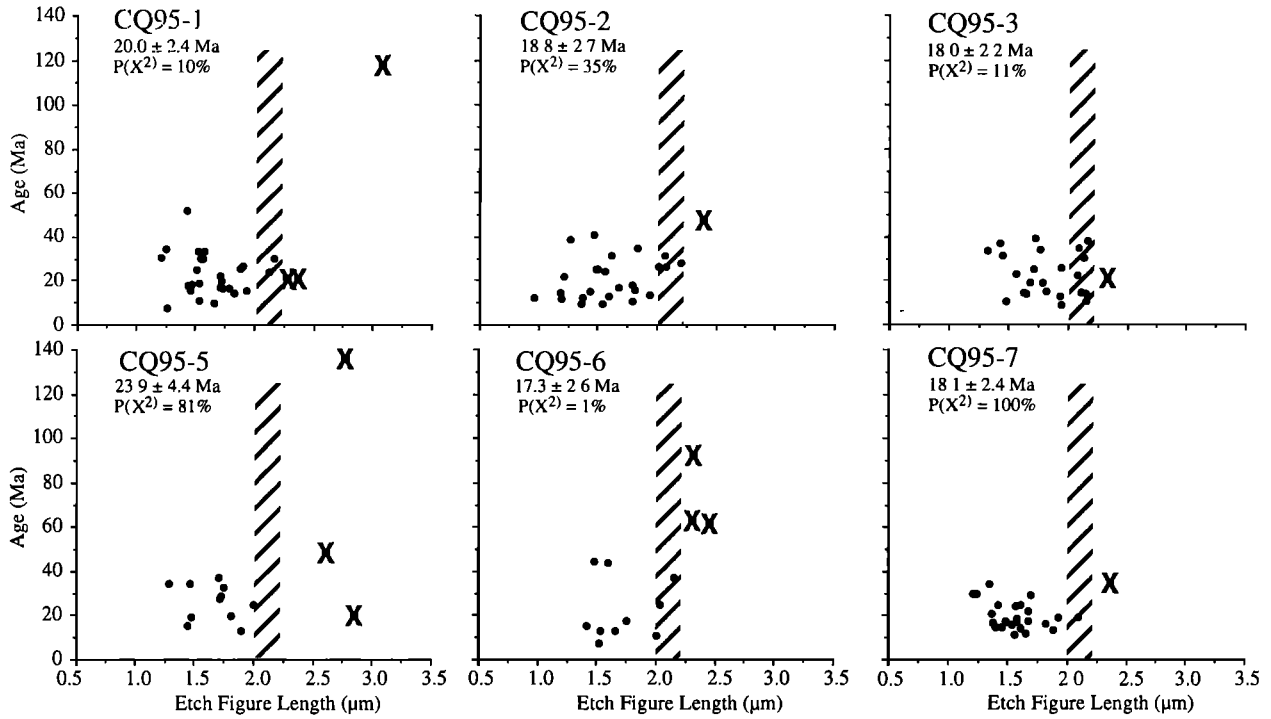

Figure 3. Plots of single-grain fission track age versus mean etch figure length. The mean etch figure length is an average of three to four etch figures of subvertical tracks measured from each apatite grain. Etch figure length is inferred to be partly controlled by the chlorine concentration of the grains analyzed; that is larger etch figure lengths correspond to greater chlorine concentration [*Donelick*, 1993; *Burtner et al.*, 1994]. The diagrams illustrate the systematic relationship between age data and compositional variations in multicompositional individual samples. All Neoproterozoic and Cambrian apatite fission track ages (Table 1) were calculated for (F, Cl, OH)-apatite populations only, omitting large D_{par} high-Cl grains (crosses) which retain older and higher temperature age information. Ages given in diagrams are central ages of (F, Cl, OH)-apatite population only. The hatched area (etch figure lengths ~2-2.3 μm) corresponds to the compositional transition between small D_{par} (F, Cl, OH)-apatites and large D_{par} Cl-apatite grains [*Burtner et al.*, 1994]. The same criteria were applied to confined track length data (see Figure 5).

etched using etching conditions of *Donelick et al.* [1999], in order to assess the influence of kinetic variability and to graphically separate large D_{par} Cl-apatite and small D_{par} (F, Cl, OH)-apatite populations. D_{par} values were measured for all 12 Neoproterozoic and Cambrian samples and most of these samples (except 97BR001) contain few of Cretaceous single-grain ages with large etch figure lengths (Figure 3). However, the structurally deepest sample from the lower Oak Creek area (CQ95-3) contains several large D_{par} apatite grains that yield Miocene single-grain ages that are statistically identical to ages from apatites with small D_{par} values (Figure 3). This observation implies that apatites from the deepest structural levels exposed along the western range flank were completely reset independent of their composition and annealing kinetics, indicating temperatures of $\geq$ 150°C.

In order to avoid compositional effects, single-grain ages characterized by large D_{par} values were not included in the calculations of apparent fission track ages for the twelve Neoproterozoic and Cambrian samples (Table 1). The older age population that is characterized by large D_{par} values can be graphically distinguished using a radial plot, which is used to isolate different fission track age populations in a suite of single-grain ages [*Galbraith*, 1990]. Figure 4 shows a radial plot of all single-grain ages from 12 Neoproterozoic and Cambrian samples. Approximately 95% of the grains cluster tightly around an age of ~18.6 Ma, while ~5% plot as outliers with a much older average of ~100 Ma.

Because of the relatively small apatite yields and young ages, the sample mounts used for age determinations yield insufficient horizontal confined track lengths to permit useful track length data to be collected. Additional apatite grain mounts were made from six samples and exposed to a ^{252}Cf fission fragment source under vacuum and subsequently etched in order to reveal more spontaneous confined tracks [*Donelick and Miller*, 1991; *Donelick et al.*, 1992] (Figure 5). The observed mean track lengths from these additional mounts are listed in Table 1. D_{par} measurements were also carried out to investigate the influence of kinetic variability on track length distributions. Comparison of the track length data from the two different D_{par} populations suggests that mean track lengths are often statistically indistinguishable, but that length distributions exhibit small differences (Figure 6). (F, Cl, OH)-apatite lengths are characterized by symmetric and unimodal distributions with a mode that tends to be slightly shorter than the mode of the Cl-apatite lengths, whereas the Cl-apatite lengths are characterized by broader

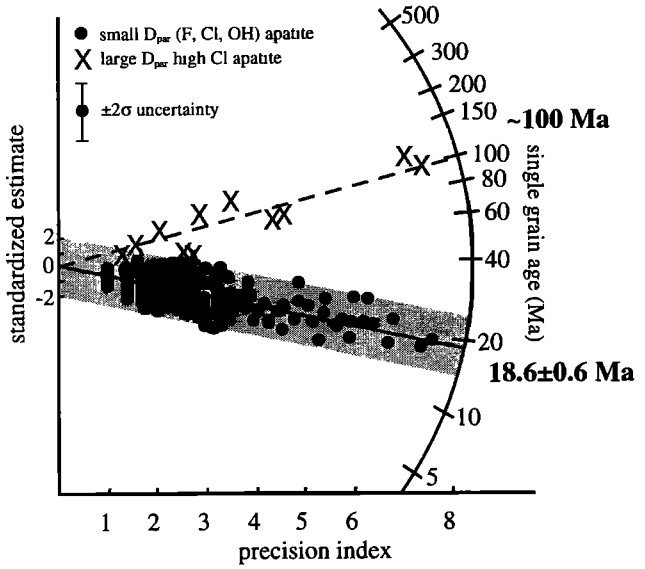

Figure 4. Radial plot of combined apatite fission track single-grain ages from all 12 Neoproterozoic and Cambrian samples of the Canyon Range, Utah. In radial plots, grain ages are read by projecting a line from the origin through the data point onto the radial age scale [*Galbraith*, 1990]. All grains in radial plots have error bars of equal length, and grains with more precise ages plot farther to the right. If single-grain ages are statistically concordant, grains cluster within a ±2σ wide swath. Radial plots are useful for graphically separating and displaying different age populations in a suite of single-grain ages. Large D_{par} high-Cl single-grain ages plot as outliers relative to the rest of the ages, which define a linear age trend with a weighted mean age of 18.6±0.6 Ma. Tight clustering of all single-grain ages in the plot indicate that the entire Canyon Range footwall block cooled very rapidly starting at ~19 Ma. The older, large D_{par} high-Cl population defines an older age trend of ~100 Ma, which appears to correlate with earlier cooling in response to thrusting in the Sevier fold and thrust belt.

and negatively skewed distributions owing to the occurrence of a few track lengths between 9 and 12 μm. These short track lengths (<12 μm) come from high Cl-apatites with etch figure diameters >3.0 μm, suggesting that those high-Cl apatite grains were partially annealed before rapid cooling in the Miocene or were more likely to preserve a partially annealed Cretaceous thermal signal (Figure 6).

The Neoproterozoic and Cambrian samples from along the western range front and from the east-west transect across the Canyon Range at Oak Creek yield statistically concordant apparent ages (Figure 7) with a weighted mean age of 18.6 ± 0.6 Ma. The samples from the western and central Canyon Range are characterized by long mean track lengths, ranging from 13.3 to 14.2 μm, indicating that these rocks underwent rapid cooling starting at ~19 Ma. A clast of Mutual Formation collected from a conglomerate in the Oak City Formation to the west of Oak Creek yields an age of 20.3 ± 6.0 Ma, statistically concordant with ages obtained from the Neoproterozoic and Cambrian bedrock samples.

Three samples from Cretaceous synorogenic conglomerates from the northeastern Canyon Range yield substantially older apatite fission track apparent ages ranging from 96.8 ± 10.6 to 41.7 ± 4.7 Ma (Figure 7). The ages of these three samples were calculated using all single-grain age data, including large D_{par} grains. Apparent ages appear to increase systematically and continuously from ~18 to ~97 Ma from west to east with increasing distance from the western range front, exposing an exhumed, east tilted Miocene partial annealing zone (Figure 7).

3.3. Apatite Fission Track Modeling

Observed track length distributions and age data were modeled with the program Monte Trax [*Gallagher*, 1995] using the experimentally derived (F, Cl, OH)-apatite annealing data of *Laslett et al.* [1987]. Model-predicted apatite fission track parameters obtained from thermal histories generated by Monte Carlo-style simulations are compared to the observed fission track data. In this study, (F, Cl, OH)-apatite age and track length data were modeled in order to constrain the thermal history and the exhumation of the Canyon Range in a more quantitative fashion. Only age and track length data from (F, Cl, OH)-apatite with D_{par} values of <2.0 μm were used in the model simulations. No large D_{par} high-Cl grains were observed in sample 97BR001, so all available length data could be included in the fission track modeling. Figure 8 shows two examples of fission track modeling results representative of the western and central Canyon Range. The results corroborate the inference based on the track length distributions that the Canyon Range underwent rapid cooling and exhumation in the early to middle Miocene. All model runs for individual samples yield consistent estimates for the timing of exhumation between ~19 and 15 Ma. The modeling results are discussed in detail in section 5.

4. Exhumation During Mesozoic Sevier Thrusting

In Cretaceous time the Canyon Range thrust sheet underwent significant deformation and exhumation as a result of motion along the PVT in late Aptian to Albian time (~115-98 Ma) [*DeCelles et al.*, 1995]. In particular, the formation of antiformal duplexes along the Pavant thrust probably caused folding of the CRT and exhumation of the overlying thrust sheet [*Sussman*, 1995]. This is supported by microstructural observations [*Mitra et al.*, 1994; *Sussman*, 1995] that indicate rocks in the Canyon Range underwent deformation and folding at relatively shallow depths (<2 km) during progressive Cretaceous unroofing. This suggests that the Canyon Range and Pavant thrust sheets must have been deeply eroded before subsequent reburial by several kilometers of wedge-top sediments of the Canyon Range Formation during Late Cretaceous to early Tertiary eastward propagation of thrusting [*Royse*, 1993; *DeCelles et al.*, 1995; *Lawton et al.*, 1997].

Apatite fission track single-grain ages from pre-Mesozoic rocks that are characterized by large D_{par} values yield ages of ~100 Ma (Figure 4). These grains were partially or not at all reset during subsequent reburial and appear to record the

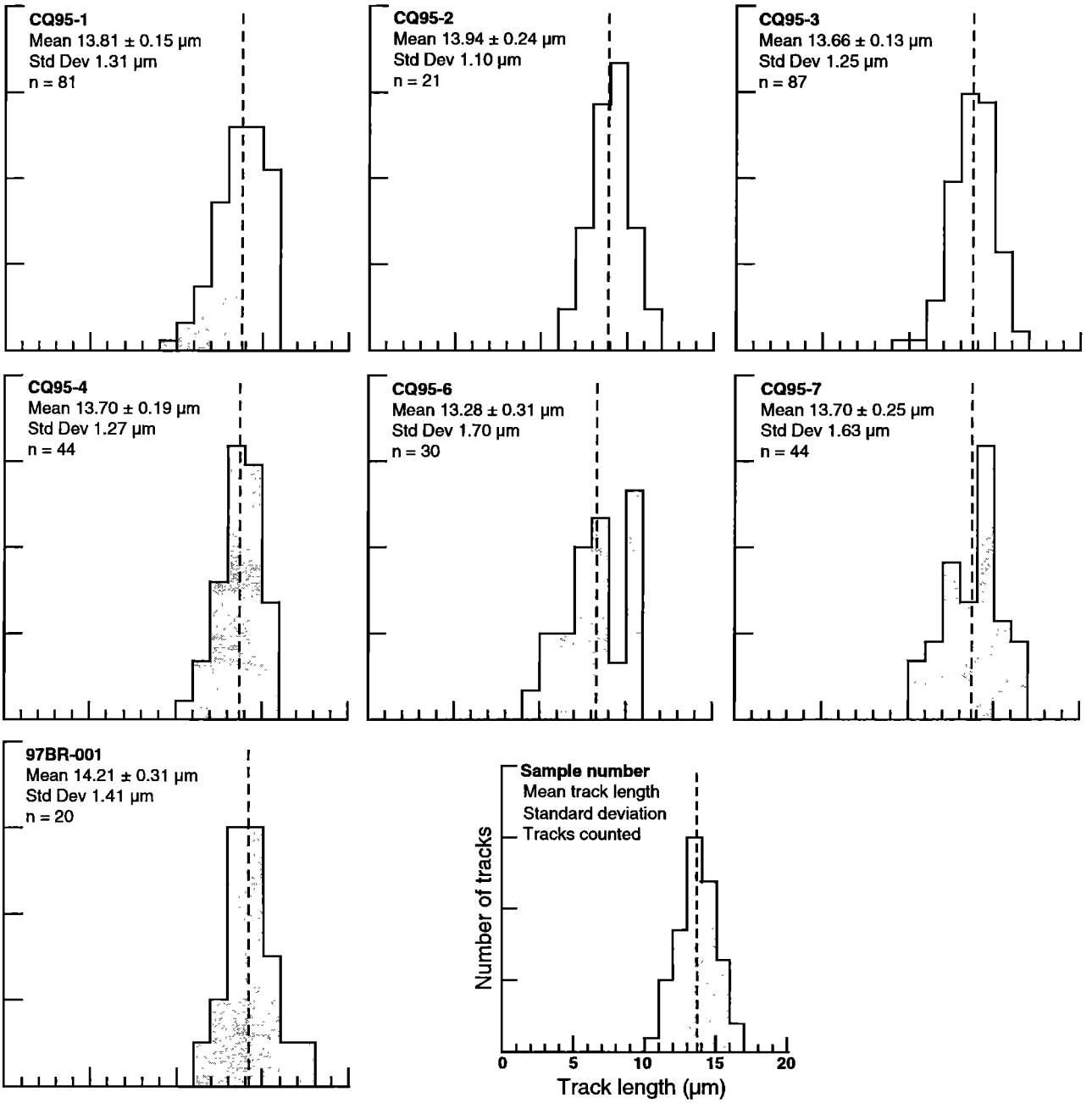

Figure 5. Apatite fission track length distributions of ^{252}Cf-exposed samples (CQ) and one sample (97BR001) used for age determination from the western and central Canyon Range illustrating the long mean track lengths indicative of rapid cooling and exhumation. All lengths are shown, independent of apatite composition. See Figure 6 for length distributions with respect to different Cl contents and Figure 8 for fission track modeling results and more quantitative treatment of the Cenozoic cooling history of the Canyon Range.

timing of erosional unroofing of the Canyon Range and Pavant thrust sheets in response to motion along the underlying PVT. This is consistent with independent estimates for the onset of subsequent wedge-top sedimentation and deposition of the Canyon Range conglomerate starting in Cenomanian times (~95 Ma) [*DeCelles et al.*, 1995]. Samples from portions of the Canyon Range conglomerate in the northeastern Canyon Range record an even more complete unroofing history of the Canyon Range thrust sheet. Multicompositional apatite fission track data from quartzite cobbles within the Canyon Range conglomerate (samples CC95-1, CC95-2, and CC95-3) were modeled by *Ketcham et al.* [1996]. Their modeling results indicate that the Canyon Range thrust sheet underwent a two-

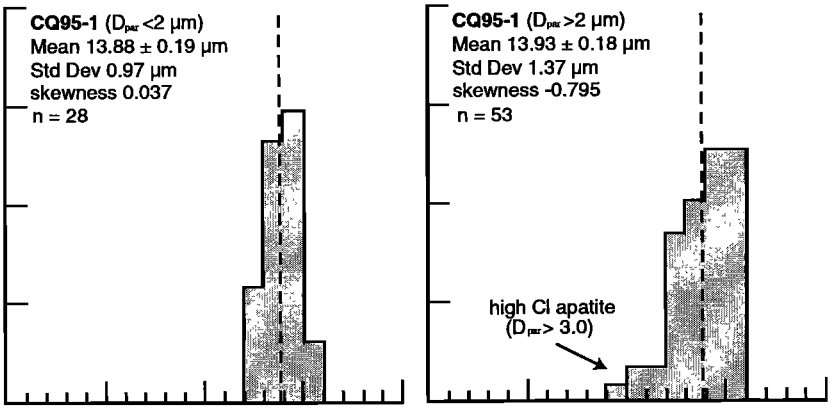

Figure 6. Representative apatite fission track length distributions of (F, Cl, OH)-apatite (etch figure width (D_{par}) < 2 μm) and Cl-apatite (D_{par} >2 μm) from a sample (CQ95-1) in the central Canyon Range. Small D_{par} (F, Cl, OH)-apatite lengths exhibit a unimodal and symmetric distribution, whereas large D_{par} Cl-apatite lengths are characterized by a negatively skewed distribution, as a result of track shortening and partial annealing of high-Cl apatite grains.

stage Cretaceous cooling history in response to cooling and exhumation associated with first thrusting along the CRT (~146 Ma) and subsequently with thrusting along the PVT (~100 Ma) [*Linn*, 1998; this study].

The presented fission track data also have interesting implications for the reconstruction of the thrust belt in the Canyon Range region. Whereas large D_{par} apatites from samples below the depositional contact of the Canyon Range conglomerate are not fully or only partially reset, small D_{par} apatites are totally annealed. This observation allows us to quantify the maximum post 100 Ma burial temperature and to estimate the amount of Cretaceous and Tertiary sediment deposited on top of the deeply eroded Canyon Range and Pavant Range thrust sheets. Assuming a geothermal gradient of ~25°C and a mean annual surface temperature of 10° ± 5°C, estimated maximum burial temperatures of ~110°-130°C would require ~4-4.5 km of Cretaceous and Tertiary overburden prior to Tertiary unroofing. These new thermochronological constraints and published stratigraphic information [e.g., *Lawton et al.*, 1997] contradict the

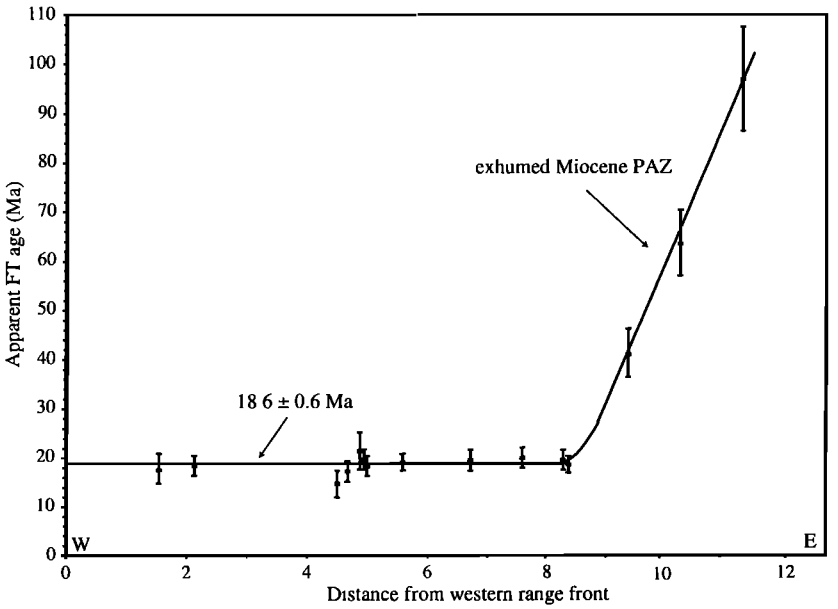

Figure 7. Diagram of apparent apatite fission track ages plotted against horizontal east-west distance measured from the western range front of the Canyon Range. Apatite fission track ages within 8 km of the range front are essentially invariant and indicate major cooling and fault slip along the Sevier Desert Detachment (SDD) starting at ~19 Ma. The weighted mean of these completely reset samples yields an age of 18.6 ± 0.6 Ma. Three partially annealed samples from the eastern flank of the Canyon Range define an exhumed partial annealing zone (PAZ).

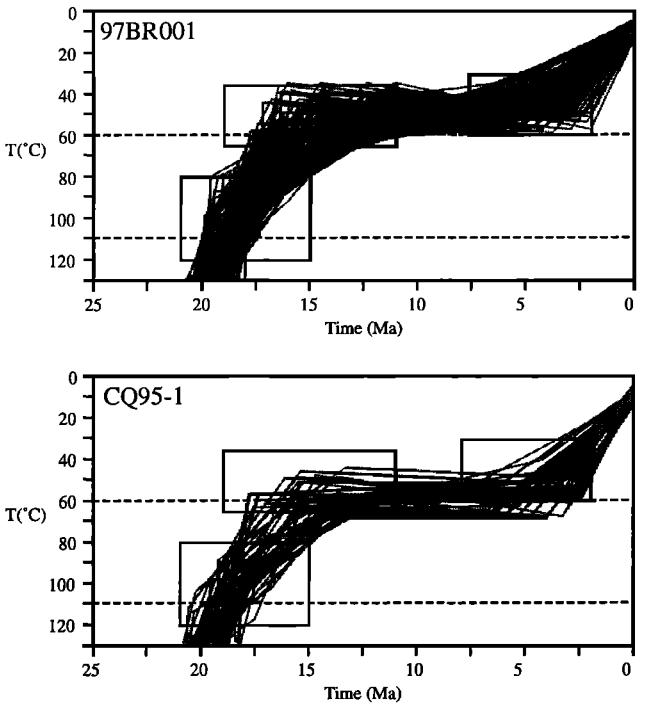

Figure 8. (F, Cl, OH)-apatite fission track modeling results of two representative samples from the central Canyon Range. Modeling results for both samples illustrate rapid cooling and exhumation of the Canyon Range between ~19 and 15 Ma. The suggested cooling rates (~10-20°C/m.y.) are inconsistent with erosional denudation and strongly support cooling because of tectonic unroofing of the Canyon Range related to motion along the Sevier Desert Detachment fault. Note that this modeling does not constrain cooling history at temperatures >110°C (all tracks in (F, Cl, OH)-apatite erased).

assessment of *Wills and Anders* [1999], who suggested that the Canyon Range did not experience substantial late Cretaceous and early Tertiary reburial.

5. Tertiary Exhumation of the Canyon Range

5.1. Unroofing History of the Canyon Range

Apatite fission track age data and fission track modeling results from the Canyon Range constrain the timing and magnitude of cooling in response to extensional unroofing subsequent to Late Cretaceous and early Tertiary reburial. The data indicate that the range underwent rapid exhumation between ~19 and 15 Ma (Figure 8). The rapid cooling rate is evidenced by the observed long and unimodal track length distributions and by the fission track modeling results, which suggest that pre-Mesozoic rocks from near the western range front cooled from $\geq$ 150°C to ~50°C during that time interval. The preextensional Miocene paleogeothermal gradient for the northern Basin and Range province is estimated at ~25°C/km and appears to be regionally uniform across much of the province [*Stockli*, 1999]. Given this pre-extensional geothermal gradient and assuming a mean annual surface temperature of 10° ± 5°C, the observed amount of cooling ($\geq$ 140°C) translates into $\geq$5.6 km of extensional unroofing between ~19 and 15 Ma and a vertical exhumation rate of ~1.4 mm/yr for the structurally deepest samples. Apparent fission track ages increase systematically from 18 to ~97 Ma west to east with increasing distance from the western range front (Figure 7). This systematic trend in apparent ages is consistent with the existence of an exhumed east tilted Miocene PAZ along the eastern flank of the Canyon Range (Figure 9). Asymmetric eastward tilting of the Canyon Range is also evident from the fact that the structurally deepest levels (antiformal duplex in the Pavant thrust sheet) outcrop along the western flank and that the structurally shallowest levels (synorogenic Canyon Range Formation) are exposed to the east of the range. This spatial distribution of fission track ages suggests that extensional unroofing of the Canyon Range was accommodated by a top down to the west normal fault along the western range flank (Figure 7).

These apatite fission track data allow us to critically evaluate the competing tectonic models for the Tertiary unroofing of the Canyon Range and its implications for the evolution of the adjacent Sevier Desert basin. A simple horst model for the Canyon Range first proposed by *Campbell* [1979] and later by *Holladay* [1984] and recently revived by *Wills and Anders* [1999] suggests that uplift of the range is controlled on both flanks by high-angle normal faults with ~1.2 and ~1.5 km of fault offsets. However, these faults by themselves can only account for a fraction of the observed extension-induced cooling, although the present physiography of the range is in part controlled by these younger high-angle normal faults that give it the appearance of a symmetrical horst block. However, the initial large-magnitude unroofing of the Canyon Range cannot be wholly ascribed to those high-angle normal faults but requires a moderately west dipping normal fault along the western range flank in order to accommodate the $\geq$5.6 km of exhumation documented above. Given this observed magnitude of footwall exhumation, a 60° high-angle normal fault would need to accommodate $\geq$6.5 km of normal slip. Such a scenario would likely result in a large half graben along the western range front and in significant footwall rotation, inconsistent with geological and geophysical data. In fact, geometric constraints on fault bedding cutoff angles argue against a high-angle normal fault and suggest a west dipping normal fault with an initial dip of 35°-40°. The easiest way of accommodating the required fault slip is to feed displacement into a low-angle detachment fault to the west of the Canyon Range as suggested by *Otton* [1995] and *Coogan and DeCelles* [1996].

In light of this, we propose a tectonic model that takes into account the geometric relationships in the Canyon Range, the constraints on timing of faulting, and magnitude of exhumation and that honors the entire cooling history of the Canyon Range (Figure 10). Our model for the tectonic evolution of the Canyon Range is characterized by (1) rapid early to middle Miocene cooling and exhumation of the Canyon Range as the breakaway region of the SDD starting at ~19 Ma and (2) subsequent small-magnitude, high-angle normal faulting along the eastern and western flanks of the Canyon Range giving the range a horst appearance and overprinting the SDD breakaway. The small degree of post

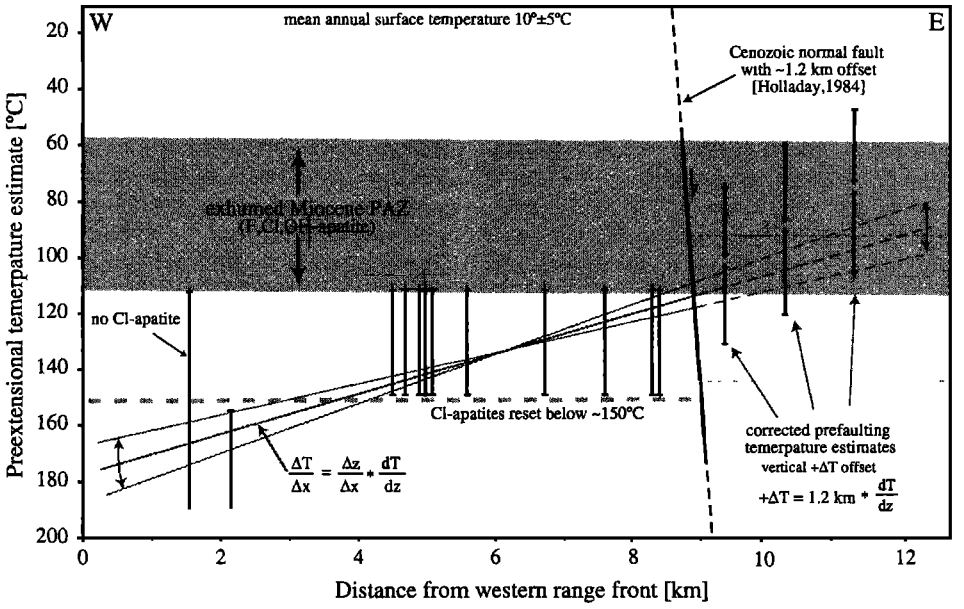

Figure 9. Diagram shows preextensional temperature estimates derived from multicompositional apatite fission track data plotted against distance from western flank of the Canyon Range. Temperature estimates for the three easternmost samples are corrected for ~1.2 km of offset along the eastern range-bounding normal fault [*Holladay*, 1984]. Assuming a geothermal gradient, preextensional temperature estimates serve as a proxy for structural depth and can be used to calculate the amount of footwall tilting. Given a geothermal gradient (dT/dz) of ~25°C/km, the systematic spatial trend in temperatures ($\Delta T/\Delta x$) translates into ~15°-20° of footwall tilt.

15 Ma uplift of the range is also suggested by the fission track modeling results and is consistent with the displacement estimates for the high-angle normal faults along both range fronts (Figure 8).

5.2. Flexural Tilting of the Canyon Range

Multicompositional apatite fission track data allow us to estimate the preextensional temperatures experienced by each sample. The geographic distribution of these temperature estimates permits us to constrain the amount of footwall tilting in the Canyon Range (Figure 9). The structurally lowest sample (97BR001) does not contain any large D_{par} Cl-apatite, but the total resetting of all (F, Cl, OH)-apatite prior to Miocene exhumation indicates that the sample resided at temperatures $\geq$110°C before extension. The deepest multicompositional sample from near the mouth of Oak Creek contains completely reset Miocene (F, Cl, OH)- and Cl-apatite, indicating temperatures $\geq$150°C (Figure 9). In contrast, samples from the central and western Canyon Range show a different behavior, with (F, Cl, OH)-apatite recording Miocene cooling and Cl-apatite only partially or not at all reset, suggesting that these samples resided in a relatively narrow preextensional temperature window between ~110° and $\geq$150°C (Figure 9). In addition, partially annealed samples from the Canyon Range conglomerate in the eastern foothills allow the estimation of preextensional temperatures decreasing from ~80° ± 10°C to about 60° ± 10°C up section. The amount of footwall rotation can be estimated from the systematic increase in maximum burial temperatures from west to east, assuming a steady state geothermal gradient and horizontal preextensional isotherms (Figure 9). For simplicity, we ignore small differences in elevation between individual samples, a reasonable assumption given the limited topographic relief along our sampling transect across the Canyon Range (Table 1).

Assuming a geothermal gradient, these preextensional temperature estimates can be used as a proxy for structural depth exposed in the footwall block (Figure 9). Thus the slope of the line $\Delta T/\Delta x$ that is defined by the preextensional temperature estimates as a function of distance from the western range front (Figure 9) is given by:

$$\frac{\Delta T}{\Delta x} = \frac{\Delta z}{\Delta x}\frac{dT}{dz}, \qquad (1)$$

and the amount of footwall tilting Φ is given by,

$$\Phi = \sin^{-1}\left[\frac{\Delta T}{\Delta x}\frac{dz}{dT}\right], \qquad (2)$$

where T is the preextensional burial temperature, x is horizontal distance measured perpendicular to the western range front, dT/dz is the estimated geothermal gradient, and z is the structural depth. A geothermal gradient of ~25°C suggests 15°-20° of eastward tilting of the Canyon Range in response to rapid exhumation between ~19 and 15 Ma, given a $\Delta T/\Delta x$ value of ~8°C/km (Figure 9).

This amount of tilting is consistent with the simple observation that structurally deeper levels outcrop along the western range flank and the structurally shallowest levels are exposed to the east of the range, suggesting an east tilted crustal section. The tilting estimate is also supported by the

geometry of Mesozoic contractional structures and by the attitude of the postthrusting Canyon Range conglomerate along the eastern flank of the range [e.g., *Lawton et al.*, 1997].

5.3. Initial Geometry of the SDD Breakaway

If one assumes that the contact between the Tertiary Oak City Formation and the underlying pre-Mesozoic strata is indeed the SDD as suggested by *Otton* [1995], then knowing the amount of flexural footwall rotation (15°-20°) from unloading allows us to estimate the initial fault angle of the SDD in the Canyon Range breakaway region. The basal contact of the Oak City Formation dips ~18°-24°, implying that the SDD had an initial dip of ~33°-44°. One arrives at similar initial fault dip estimates by projecting the KT conglomerates on the east side of the range upward, which *Otton* [1995] demonstrated (Figure 2). The initial fault trajectory of the SDD, based on the cutoff angle between the fault and the postthrusting early Tertiary conglomerates, is ~40°-45°. Furthermore, if the initial trajectory of the detachment is drawn on the restored preextensional section such that the base of the Tintic appears in the footwall, an initial dip of 35°-45° is achieved, suggesting that the SDD initially cut obliquely (~40°) across an upright (vertical) antiform-synform pair in the breakaway region (Figures 10 and 11).

The geometry of the Cricket Range can be reasonably inferred from the surface geology and geophysical data, which indicate a low-angle hanging wall cutoff by the detachment and a subparallelism between pre-Mesozoic and early Tertiary strata. The hypothesized footwall cutoff in the Canyon Range is the steeply dipping CRT, creating a possible incompatibility between hanging wall and footwall geometries. However, an initial fault dip of ~35°-40° combined with ~20° of flexural footwall rotation of the Canyon Range and ~25°-30° of eastward tilting of the Cricket Mountains due to hanging wall rollover allow the reconciliation of potential incompatibilities when restoring the preextensional geometry of the breakaway and suggest that the Canyon Range syncline was originally a relatively upright fold prior to Tertiary tilting (Figure 10).

5.4. Tertiary Oak City Formation and Fool Creek Conglomerate

As discussed above, *Otton* [1995] assigned a tentative Miocene age to the Oak City Formation, but this ~12 Ma age most likely represents a minimum age for the conglomerates

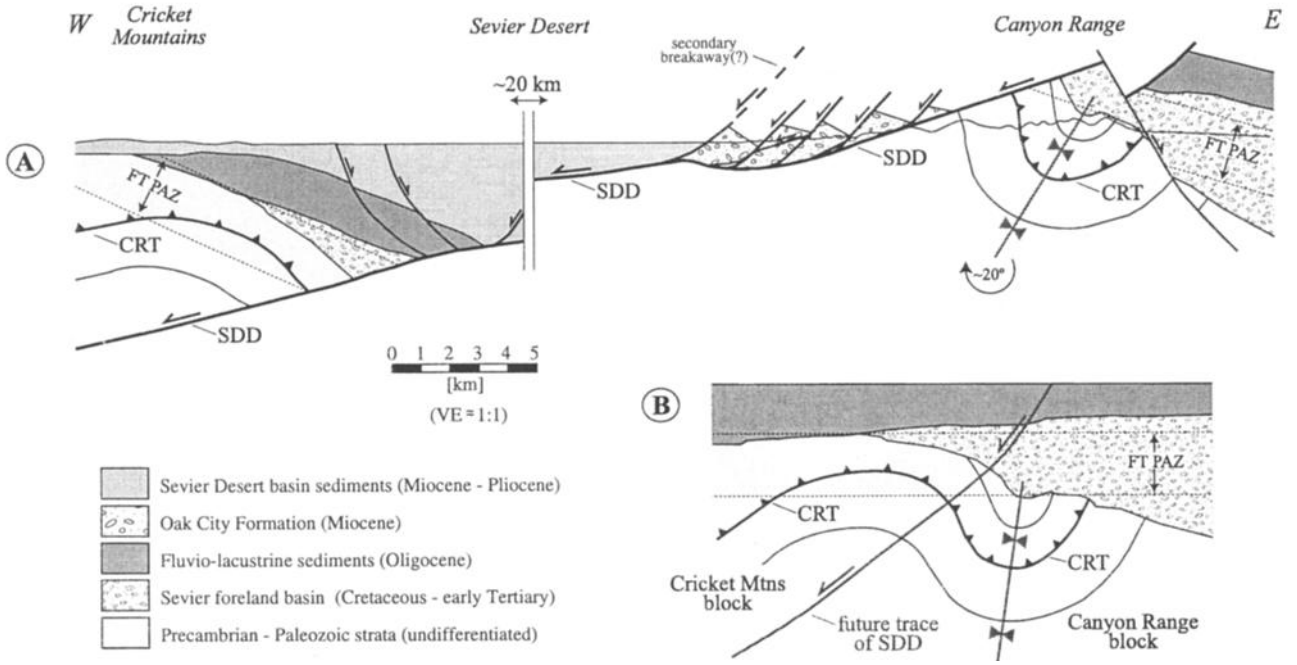

Figure 10. Simplified tectonic cross sections of the central Sevier Desert basin. (a) Present-day geometry of the Canyon Range and Cricket Mountains. Separation of Canyon Range thrust (CRT) cutoffs in the Cricket Mountains and Canyon Range indicates ~45 km of normal faulting along the SDD. Depth to SDD east of the Cricket Mountains block is taken from *Von Tish et al.* [1995]. The geometry of the fossil, preextensional apatite fission track partial annealing zone (FT PAZ) illustrates the amount of flexural footwall rotation of the Canyon Range and hanging wall rollover in the Cricket Mountains block in response to fault slip along the SDD. (b) Restored post-Mesozoic contractional geometries of the Canyon Range and Cricket Mountains blocks prior to inception of extensional faulting (late Oligocene). The reconstruction indicates that the synform in the Canyon Range and the antiform in the Cricket Mountains formed an upright fold pair that was cut obliquely by the SDD at an initial fault angle of ~35°-40°. Thickness of Eocene–Oligocene overburden is estimated from multicompositional fission track data (see text for details).

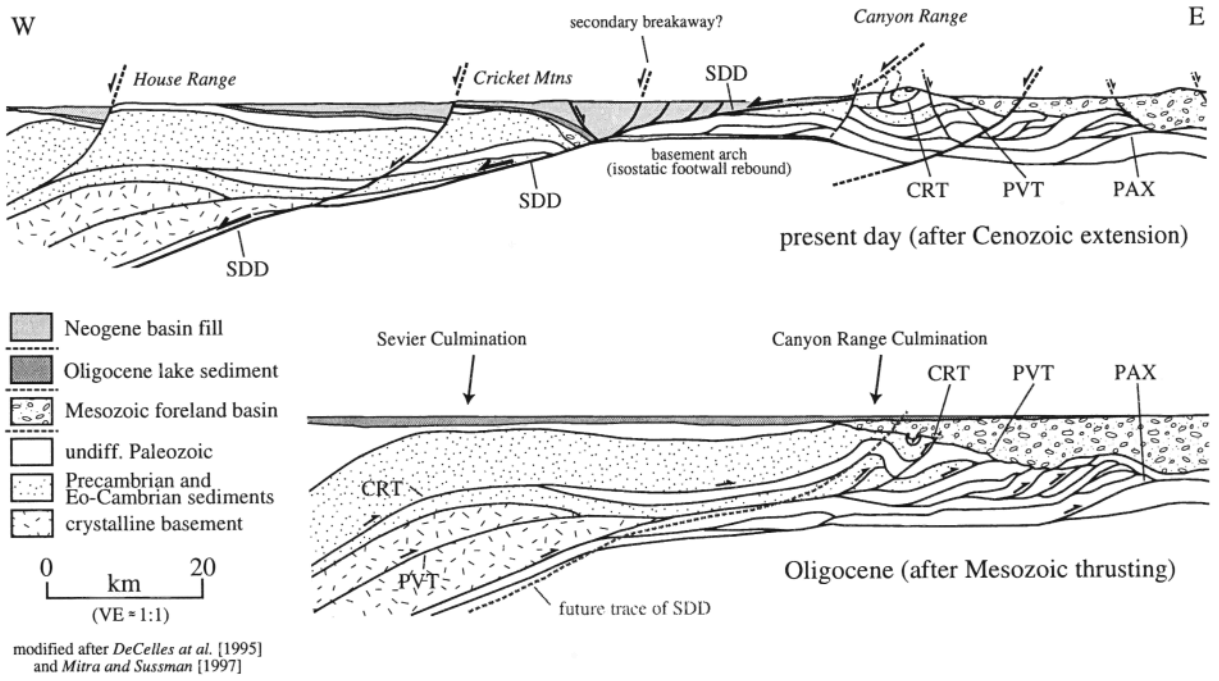

Figure 11. Cross sections of the Canyon Range–Sevier Desert area in west-central Utah, illustrating the Mesozoic and Cenozoic kinematic history. Thrusts shown on cross sections are the Canyon Range (CRT), Pavant (PVT), and Paxton (PAX) thrusts. Rocks in the Canyon Range were uplifted and eroded during Mesozoic thrust faulting (~130-90 Ma) as constrained by synorogenic sedimentary deposits and apatite fission track results [*Ketcham et al.*, 1996; this study]. In the early to middle Miocene (~19-15 Ma) the Canyon Range underwent rapid cooling and exhumation. The tectonic unroofing of the Canyon Range is attributed to footwall uplift in response to motion along the Sevier Desert Detachment.

in the Oak City Formation. An apatite fission track age from a clast of the Mutual Formation collected from the Oak City Formation yields a maximum age for the conglomerate of 20.3 ± 6.0 Ma. This brackets the depositional age of the Oak City conglomerates between ~20 and ~12 Ma, implying that they are synextensional sediments that were deposited in a supradetachment basin in the SDD breakaway zone [*Otton*, 1995; *Morris and Hebertson*, 1996] (Figure 10).

The enigmatic Fool Creek conglomerate (Figure 1) has historically influenced many working hypotheses for the tectonic evolution of the Canyon Range [*Wills and Anders*, 1999]. *Campbell* [1979] correlated the poorly exposed and crudely bedded conglomerates outcropping near the top of the range with basal units of the Oak City Formation and assigned a tentative Oligocene age. In contrast, *Otton* [1995] argued that the conglomerates, infilling modern drainages, are much younger than Oligocene and, in fact, are younger than the Miocene Oak City Formation. Although the unit so far has not been directly dated, the exhumation history of the pre-Mesozoic strata in the Canyon Range sheds new light on the potential age of the deposit. An Oligocene age for the Fool Creek conglomerate is unlikely since the thermochronological data indicate that pre-Mesozoic rocks were buried under >4-4.5 km of overburden prior to the onset of Miocene exhumation. Therefore we suggest that the poorly exposed and poorly consolidated Fool Creek conglomerate substantially postdates unroofing of the range. It most likely represents erosional remnants of Pliocene-Pleistocene(?) alluvium reworked from the Canyon Range conglomerate and might be correlative with alluvium unconformably overlying the Oak City Formation [*Otton*, 1995].

6. Implications for Detachment Faulting Along the SDD

6.1. Timing Constraints on the SDD

Temporal constraints on the onset of faulting in the Sevier Desert basin are based on subsurface Eocene to Oligocene deposits from ~2 km depth in the Gulf Gronning well near the western margin of the basin [*Lindsey et al.*, 1981]. Palynological and zircon and apatite fission track age data indicate an Oligocene age of ~28-26 Ma. *Mitchell and McDonald* [1987] suggested the presence of an additional ~2 km of pre-28 Ma sediments below the dated lacustrine and volcanic sediments and speculated that the oldest sediments may be as old as Eocene. These 28-26 Ma deposits rest unconformably on Paleozoic and Precambrian rocks and dip 18°-25° to the east, with no fanning geometries or thickness changes evident in seismic data [*Von Tish et al.*, 1985] (Figure 10). This has led most studies to conclude that faulting in the Sevier Desert and extensional faulting along SDD began after late Oligocene time [*Lindsey et al.*, 1981; *Mitchell and McDonald*, 1987; *Coogan and DeCelles*, 1996].

This conclusion is also supported by the fact that Oligocene fluvio-lacustrine sediments in the Sevier Desert region are not limited to the basin but outcrop outside of the basin along the east tilted eastern flank of the House Range [*Hintze*, 1981] (Figure 11). Exposures of Eocene to Oligocene fluvio-lacustrine sediments and intercalated volcanic tuffs occur throughout the eastern Great Basin and appear to represent remnants of regionally extensive, long-lived lake systems that covered a large proportion of the eastern Great Basin [*Gans and Calvert*, 2000]. Deposition of these Eocene to Oligocene lake sediments is thought to be the result of regional postcollisional subsidence [*Wills and Anders*, 1999] or of crustal thinning during localized Eocene to Oligocene extension and crustal collapse in the eastern Great Basin [e.g., *Gans*, 1987; *Miller et al.*, 1999; *Gans and Calvert*, 2000].

The fission track data presented from the breakaway zone of the SDD corroborate the post-Oligocene onset of faulting and directly date the onset of footwall exhumation and large-magnitude displacement along the SDD starting at ~19 Ma. The timing appears to be consistent with the onset of major extensional faulting in the northernmost Sevier Desert region. For example, in the Drum Mountains (Figure 1), *Lindsey* [1982] documented a prominent angular unconformity between the 21.3 Ma Spor Mountain rhyolite and the 6.3 Ma Topaz Mountain rhyolite, suggesting that the major extension occurred between 21.3 and 6.3 Ma.

Thus it appears that 28-26 Ma lacustrine sediments found in the subsurface of the Sevier Desert basin predate extension along the SDD and do not constrain the onset of extension. Therefore the fission track data do not imply a time lag of ~8 m.y. between the onset of slip along the SDD and the initial exhumation of the breakaway in the Canyon Range, as suggested by *Wills and Anders* [1999]. Rather, the timing of exhumation of the breakaway of the SDD in the Canyon Range as constrained by apatite fission track dating directly dates the inception of major extensional faulting along the SDD as beginning ~19 Ma.

Reported late Miocene zircon fission track ages of 10.8 ± 0.9 and 13.0 ± 1.0 Ma and an apatite fission track age of 5.8 ± 2.2 Ma from subsurface samples in the western portion of the Sevier Desert [*Allmendinger and Royse*, 1995] are considerably younger than apatite fission track ages from the Canyon Range, implying that lowerplate rocks beneath the western Sevier Desert basin cooled later than rocks in the breakaway zone. This observation might point to progressive unroofing of the SDD lower plate either in a rolling hinge setting [e.g., *Buck*, 1988; *Hamilton*, 1988; *Wernicke and Axen*, 1988] or simply due to progressive unroofing along the west dipping low-angle SDD [*Wernicke*, 1981]. It might also suggest the existence of secondary breakaway zones in the central Sevier Desert and the progressive abandonment of the primary breakaway in the Canyon Range during continued slip after ~15 Ma (Figure 10). Such a scenario would explain the position of the broad basement arch beneath the Sevier Desert to the west of the Canyon Range, which has been attributed to isostatic footwall rebound [e.g., *DeCelles et al.*, 1995] (Figure 11). Post-15 Ma slip along the SDD would also be consistent with the presence of late Miocene synextensional sediments in the Sevier Desert basin and with paleoseismologic and GPS data indicating continued extension along the SDD (Niemi et al., in preparation, 2001).

The subsurface fission track data reported by *Allmendinger and Royse* [1996] are difficult to evaluate quantitatively because of the lack of apatite track length data. Such data would be particularly important since the sample might have undergone minor in situ annealing at elevated down hole temperatures at a depth of ~1900 m in the Arco Meadow Federal well. *Anders et al.* [1995] further argued that these fission track ages might have been reset owing to magmatic activity. However, such a scenario appears rather unlikely, particularly since apatite and zircon fission track ages from samples in the Gulf Gronning well in the adjacent hanging wall samples preserve their volcanic ages and do not exhibit any evidence for resetting despite their spatial proximity to a small Quaternary volcanic center [*Lindsey et al.*, 1981].

6.2. Magnitude and Rate of Fault Slip Along the SDD

The Sevier Desert basin formed as the result of low-angle normal faulting along the SDD with an estimated cumulative displacement of ~38 km [*Allmendinger et al.*, 1983; *Von Tish et al.*, 1985] or ~40-47 km [e.g., *DeCelles et al.*, 1995; *Mitra and Sussman*, 1997] based on cross-sectional reconstructions of the Mesozoic contractional edifice of the Sevier orogenic belt (Figs. 10 and 11). Knowledge of the timing and magnitude of exhumation of the Canyon Range makes it possible to estimate the time-integrated average rate of displacement along the SDD in the breakaway region, assuming a paleogeothermal gradient and subhorizontal isotherms. Using a Miocene paleogeothermal gradient estimate for the Great Basin of ~25°C/km [*Stockli*, 1999], the cooling of the Canyon Range suggests ~5.6 km of unroofing in response to slip along the SDD between ~19 and 15 Ma at a vertical rate of ~ 1.4 mm/yr. Given that the SDD in the breakaway zone appears to dip ~40°-35° to the west, the estimated unroofing of the Canyon Range translates into ~12-10 km of fault slip along the SDD between ~19 and 15 Ma at a time-integrated dip-slip displacement rate of ~2.4-2.1 mm/yr. A lower geothermal gradient estimate would result in a significant increase in fault displacement and slip rates. These estimates for the early to middle Miocene slip rate and the magnitude of displacement along the SDD likely represent minimum values since the fault dip decreases during progressive footwall rotation (~20°). Subsequent, post 15 Ma cooling rates for the breakaway zone cannot be constrained quantitatively by apatite fission track data. However, fission track modeling suggests ~1.5 km of unroofing after 15 Ma, which in part might be attributable to younger, active high-angle faulting along the present-day range front [e.g., *Wills and Anders*, 1999].

We envisage a slip history for the SDD characterized by (1) fault initiation at ~19 Ma with a minimum slip rate of ~2.4-2.1 mm/yr and (2) continued fault slip at a comparable rate of ~2.3-1.7 mm/yr, assuming that the remaining 26-35 km of total slip occurred after 15 Ma. These rate estimates agree with the maximum rates that can be ascribed to present extension across the SDD based on geodesy and paleoseismology (Niemi et al., in preparation, 2001). A constant-rate model for the Neogene with an average slip rate of ~2 mm/yr would explain the middle to late Miocene fission track ages from the subsurface of the Sevier Desert basin [*Allmendinger and Royse*, 1995], the significant post 10 Ma evolution of the basin based on rollover and faulting of late

Miocene intrabasin basalts [*Von Tish et al.*, 1985], and the active fault scarps in the middle of the basin [*Hoover*, 1974]. However, these data do not preclude a model in which slip rates vary through time. The slip estimates derived from our thermochronological data do not account for displacement along faults to the west of the Canyon Range that appear to sole into the SDD, such as along the western side of the Cricket Mountains, suggesting that the cumulative displacement along the SDD probably increases from east to west [*Wernicke*, 1981]. Early to middle Miocene slip along these faults would result in a significant increase in slip rates along the SDD during that time.

7. Extensional Faulting in the Eastern Great Basin

The constraints on the timing and magnitude of exhumation of the SDD breakaway and displacement along the SDD prove important for the understanding of extension in the eastern part of the northern Basin and Range province. Thus it is important to understand extensional faulting along the SDD in the context of the regional spatial and temporal distribution of extension in the eastern Great Basin.

Areas to the north and south of the Canyon Range appear to have undergone substantial east-west extension in Miocene time that might be kinematically linked to slip along the SDD. In the Drum Mountains at the northern edge of the north of the Sevier Desert, *Lindsey* [1982] documented extensional faulting between ~21 and ~7 Ma, on the basis of a prominent angular unconformity. It is unclear, however, whether faulting in the Drum Mountains is directly related to slip along the SDD (Figure 1). To the south of the Canyon and Pavant Ranges, the west dipping Cave Canyon detachment fault, exposed in the Mineral Mountains, projects beneath the southernmost Sevier Desert region [*Coleman and Walker*, 1994; *Coleman et al.*, 1997] (Figure 1). Thermochronological data from the central Mineral Mountains show the late Miocene batholith was exhumed during slip along the Cave Canyon detachment from ~11 Ma to the present [*Evans and Nielson*, 1982; *Coleman et al.*, 1997]. However, *Price* [1998] claimed that significant slip along the Cave Canyon detachment occurred before 11 Ma, on the basis of crosscutting relations between ~11 Ma dikes and cataclasites along the eastern segment of the Cave Canyon detachment. It is therefore possible that the Mineral Mountains underwent two periods of significant footwall exhumation between 18-11 Ma and 7.6 Ma to present. Conservative structural reconstructions of the Mineral Mountains region argue for at least 20 km and up to 30 km of east-west extension [*Walker and Bartley*, 1991; *Coleman et al.*, 1997]. The lack of evidence for an east-west accommodation zone between the Sevier Desert and Mineral Mountains domains and the similar magnitudes of extension accommodated by the SDD and the Cave Canyon detachments suggest that the two detachment faults are kinematically linked and part of the same extensional detachment system.

The eastern Great Basin west of the Sevier Desert region is dominated by an east dipping low-angle detachment fault system, the Snake Range décollement [e.g., *Miller et al.*, 1983; *Bartley and Wernicke*, 1984; *Lee et al.*, 1987] (Figure 1). The $^{40}Ar/^{39}Ar$ and fission track data from the Deep Creek Range and northern Snake Range indicate two discrete episodes of extensional fault slip and tilting in the Oligocene (37–34 Ma) and the Miocene (18–14 Ma) [*Gans et al.*, 1991; *Lee*, 1995]. Fission track data from the northern and southern Snake Ranges and sedimentary and volcanic sequences in the hanging wall of the Snake Range décollement also support a two-stage movement history [e.g., *Miller et al.*, 1999]. The data provide compelling evidence for a major episode of Miocene slip along the Snake Range décollement at ~20-16 Ma, accommodating a minimum of 12–15 km of fault slip. These data indicate that the east dipping Snake Range décollement was active at the same time as rapid fault slip occurred on the SDD. This temporal overlap of rapid extension along the Snake Range décollement and the SDD suggest that the two fault systems of opposite polarities formed a conjugate set of faults, accommodating large-magnitude east-west extension during early to middle Miocene times.

8. Conclusions

Apatite fission track results from Proterozoic and Lower Cambrian quartzites collected from the Canyon Range reveal a significant early to middle Miocene (~19-15 Ma) cooling event in response to rapid extensional unroofing. Samples from an east-west transect contain older, high Cl-apatite grains, indicating that preextensional burial temperatures were sufficient to fully reset small D_{par} (F, Cl, OH)-apatite but not large D_{par} Cl-apatite. This compositionally induced spread in single-grain ages indicates that the pre-Mesozoic rocks in the Canyon Range resided in a temperature window between ~110° and $\geq$150°C prior to Miocene exhumation. These preextensional temperature estimates suggest ~4.5 to >5.6 km of unroofing since the early Miocene, assuming a geothermal gradient around ~25°C/km.

The spatial distribution of preextensional temperature estimates across the range indicates 15°-20° of eastward tilting of the Canyon Range during rapid exhumation between ~19 and 15 Ma, assuming near-horizontal preextensional isotherms. These data suggest top down to the west extensional unroofing of the Canyon Range accommodated by a moderately low-angle, west dipping extensional structure along the western range flank with an initial dip of ~35°-40°. The data do not support the hypothesis of *Wills and Anders* [1999] that the Canyon Range was exhumed as a horst bound by major high-angle faults. Rather, these observations are consistent with rapid early to middle Miocene cooling and exhumation of the Canyon Range occurring as a result of footwall unroofing along the low-angle Sevier Desert Detachment fault and support the hypothesis that the Canyon Range is the breakaway zone of the SDD. An early Miocene fission track age from the lower part of the Oak City Formation brackets its depositional age at 20 to 12 Ma, implying that it represents Miocene synextensional sediments that were deposited in the hanging wall of the SDD in the breakaway zone. These constraints corroborate the model of *Otton* [1995] and *Coogan and DeCelles* [1996] in which the west dipping contact between the Tertiary Oak City Formation and the pre-Mesozoic strata of the western Canyon Range is the low-angle SDD. Trenching of the poorly exposed contact between the Miocene Oak City Formation

and the underlying pre-Mesozoic strata might eliminate any ambiguity concerning the nature and significance of the contact.

The thermochronological data from the breakaway zone directly date the onset of large-magnitude displacement along the SDD between ~19 and 15 Ma. Given that the SDD in the breakaway zone appears to dip ~40°-35° to the west in the Canyon Range, the estimated unroofing of the SDD breakaway translates into ~12-10 km of fault slip along the SDD at an average rate of ~2.4-2.1 mm/yr. Thus we envisage a slip history for the SDD characterized by fault initiation at ~19 Ma with a minimum slip rate of ~2.4-2.1 mm/yr and followed by continued fault slip at a rate of ~2.3-1.7 mm/yr after 15 Ma. These rates are consistent with geodetic measurements of present-day extension across the SDD (Niemi et al., in preparation, 2001). To test whether the slip rates along the SDD have been constant or have varied through time, additional thermochronological constraints such as fission track, $^{40}Ar/^{39}Ar$ K-feldspar, and (U-Th)/He titanite data would be required to comprehensively elucidate the cooling history of the SDD footwall in the subsurface east of the Cricket Mountains.

Miocene large-magnitude extension in the eastern Great Basin is not limited to the Sevier Desert region west of the Canyon Range. The Cave Canyon detachment exposed in the Mineral Mountains projects beneath the southern Sevier Desert and is characterized by up to 30 km of Miocene extension. To the west the east dipping Snake Range décollement exhibits evidence for large-magnitude extension in early and middle Miocene times, suggesting that the two fault systems may have formed a conjugate set of faults. The timing of tectonic unroofing of the Canyon Range appears to be roughly synchronous with large-magnitude extension along the Snake Range décollement and with an earlier phase of extension along the Cave Canyon detachment, pointing to widespread east-west extension in the eastern Great Basin in the early and middle Miocene. The SDD and the Cave Canyon detachment fault form a continuous north-south corridor characterized by large-magnitude Tertiary extension and figure prominently into strain estimates of the Basin and Range province as a whole [e.g., *Wernicke*, 1992].

This study presents compelling evidence for the existence of the Sevier Desert Detachment, which has been at the center of the controversy surrounding the viability of low-angle detachment faulting. Thermochronologic and geologic constraints from the SDD support that it is mechanically feasible to accommodate large-magnitude extension along a moderately low to low-angle detachment fault.

Acknowledgments. This project was supported by NSF grant EAR-9417939 (to E. L. Miller and T. A. Dumitru) and by a Geological Society of America student research grant to J. K. Linn. We thank R. Donelick for permission to use his etch figure technique and the Texas A&M and Oregon State University reactor facilities for sample irradiations. J. K. Linn would like to thank the University of Texas at Austin fission track laboratory. We also would like to thank J. Bartley, B. Currie, P. DeCelles, R. Donelick, L. Gilley, M. Hulver, S. Klemperer, T. Lawton, E. Miller, C. Naeser, J. Otton, and A. Sussman for stimulating discussions and helpful insights and B. Wernicke, D. Cowan, and M. Anders for improving the final version of the manuscript.

References

Abers, G. A., C. Z. Mutter, and J. Fang, Shallow dips of normal faults during rapid extension: earthquakes in the Woodlark-D'Entrecasteaux rift system, Papua New Guinea, *J. Geophys. Res.*, *102*, 15,301-15,317, 1997

Allmendinger, R W, and F. Royse, Is the Sevier Desert reflection of west-central Utah a normal fault?, Reply, *Geology*, *23*, 669-670, 1995

Allmendinger, R. W., J. W. Sharp, D Von Tish, L Serpa, L. Brown, S. Kaufman, J. Oliver, and R. B. Smith, Cenozoic and Mesozoic structure of the eastern Basin and Range province, Utah, from COCORP seismic-reflection data, *Geology*, *11*, 532-536, 1983.

Anders, M. H., and N. Christie-Blick, Is the Sevier Desert reflection of west-central Utah a normal fault?, *Geology*, *22*, 771-774, 1994.

Anders, M H., N. Christie-Blick, and S Wills, Is the Sevier Desert reflection of west-central Utah a normal fault?, Discussion, *Geology*, *23*, 669-670, 1995

Armstrong, R. L., Sevier orogenic belt in Nevada and Utah, *AAPG Bull*, *79*, 429-458, 1968.

Bartley, J M, and B P. Wernicke, The Snake Range decollement interpreted as a major extensional shear zone, *Tectonics*, *3*, 647-657, 1984

Boncio, P, F. Brozzetti, and G. Lavecchia, Architecture and seismotectonics of a regional low-angle normal fault zone in central Italy, *Tectonics*, *19*, 1038-1055, 2000

Buck, R W, Flexural rotation of normal faults, *Tectonics*, *7*, 959-973, 1988

Burtner, R. L, A. Nigrini, and R. A. Donelick, Thermochronology of Lower Cretaceous source rocks in the Idaho-Wyoming thrust belt, *AAPG Bull.*, *78*, 1613-1636, 1994.

Campbell, J. A., Middle to late Cenozoic stratigraphy of the Canyon Range, central Utah, *Utah Geol.*, *6*, 1-16, 1979.

Carlson, W. D., R A Donelick, and R. A. Ketcham, Variability of apatite fission track kinetics, I, Experimental results, *Am. Mineral*, *84*, 1213-1223, 1999

Christiansen, F. W., Structure and stratigraphy of the Canyon Range, central Utah, *Geol. Soc. Am. Bull.*, *63*, 717-740, 1952.

Coleman, D. S., and J. D. Walker, Modes of tilting during extensional core complex development, *Science*, *263*, 215-218, 1994.

Coleman, D. S, J. M. Bartley, J. D. Walker, D. E. Price, and A. M. Friedrich, Extensional faulting, footwall deformation and plutonism in the Mineral Mountains, southern Sevier Desert, in *Mesozoic to Recent geology of Utah*, edited by P. K. Link, *Brigham Young Univ. Geol. Stud.*, *42*, 203-233, 1997.

Coogan, J. C., P. G. DeCelles, G Mitra, and A. J. Sussman, New regional balanced cross section across the Sevier Desert region and the central Utah thrust belt, *Geol Soc. Am. Abstr. Programs*, *27*, 7, 1995.

Coogan, J. C., and P G. DeCelles, Extensional collapse along the Sevier Desert reflection, northern Sevier Desert basin, western United States, *Geology*, *24*, 933-936, 1996

Corrigan, J D., Apatite fission track analysis of Oligocene strata from South Texas, U S.A., Testing annealing models, *Chem. Geol.*, *104*, 227-249, 1993

DeCelles, P. G., T. F. Lawton, and G. Mitra, Thrust timing, growth of structural culminations, and synorogenic sedimentation in the type Sevier orogenic belt, western United States, *Geology*, *23*, 699-702, 1995.

Donelick, R. A., A method of fission track analysis utilizing bulk etching of apatite Patent 6,267,274, U.S. Patent and Trademark Office, Washington, D. C., 1993.

Donelick, R. A., R. A Ketcham, and W. D. Carlson, Variability of apatite fission track annealing kinetics, II, Crystallographic orientation effects, *Am. Mineral.*, *84*, 1224-1234, 1999.

Donelick, R. A., and D S. Miller, Enhanced TINT fission track densities in low spontaneous track density apatites using ^{252}Cf-derived fission fragment tracks: A model and experimental observations, *Nucl Tracks Radiat. Meas*, *18*, 301-307, 1991.

Donelick, R. A., S. C. Bergman, and J P. Talbot, ^{252}Cf irradiation of apatite fission track samples improves spontaneous, confined, track-in-track densities, *Paper presented at 7th International Workshop on Fission Track Thermochronology*, Philadelphia, Pa., 1992.

Dumitru, T. A., A new computer-automated microscope stage system for fission track analysis, *Nucl Tracks Radiat Meas*, *21*, 575-580, 1993.

Dumitru, T. A., Fission track geochronology, in Quaternary Geology, in *Quaternary Geochronology: Methods and Applications*, edited by J. S. Noller et al., AGU Ref. Shelf, vol 4, pp. 131-156, AGU, Washington, D C., 2000.

Evans, S. H., and D. L Nielson, Thermal and tectonic history of the Mineral Mountains intrusive complex, *Trans. Geotherm. Resour s Counc.*, *6*, 15-18, 1982

Fitzgerald, P. G , J. E. Fryxell, and B. P. Wernicke, Miocene crustal extension and uplift in southeastern Nevada· Constraints from fission track analysis, *Geology, 19*, 1013-1016, 1991.

Fleischer, R L., P. B. Price, and R. M. Walker, Nuclear Tracks in Solids, Univ. of Calif Press, Berkeley, 1975.

Foster, D. A., T. M. Harrison, C. F Miller, and K. A Howard, The $^{40}Ar/^{39}Ar$ thermochronology of the eastern Mojave Desert, California, and adjacent western Arizona with implications for the evolution of metamorphic core complexes, *J. Geophy. Res., 95*, 20,005-20,024, 1990.

Galbraith, R. F , On statistical models for mixed fission track ages, *Nucl. Tracks Radiat. Meas , 13*, 471-478, 1981.

Galbraith, R. F., and G. M. Laslett, Statistical models for mixed fission track ages, *Nucl Tracks Radiat. Meas., 21*, 459-470, 1983

Galbraith, R F , The radial plot: Graphical assessment of spread in ages, *Nucl. Tracks Radiat. Meas., 17*, 207-214, 1990.

Gallagher, K., Evolving temperature histories from apatite fission-track data, *Earth Planet. Sci. Lett , 136*, 421-443, 1995

Gans, P. B , An open-system, two-layer crustal stretching model for the eastern Great Basin, *Tectonics, 6*, 1-12, 1987.

Gans, P. B., E. L. Miller, R. Brown, G. Houseman, and G. S. Lister, Assessing the amount, rate and timing of tilting in normal fault blocks: A case study of tilted granites in the Kern-Deep Creek Mountains, Utah, *Geol. Soc. Am. Abstr Programs, 23*, 28, 1991.

Gans, P. B., and A. T. Calvert, Eocene tectonics and paleogeography of the eastern Great Basin: Inception of gravitational collapse of the late Mesozoic contractional Orogen, *Eos Trans., AGU, 81*, (48), T50F-08, Fall meet. Suppl., 2000

Gleadow, A. J. W., I. R Duddy, P. F. Green, and J. F Lovering, Confined fission track lengths in apatite: A diagnostic tool for thermal history analysis, *Contrib. Mineral Petrol., 94*, 405-415, 1986.

Green, P. F., A new look at statistics in fission track dating, *Nucl. Tracks Radiat Meas., 5*, 77-86, 1981.

Green, P. F., I. R. Duddy, A. J. W. Gleadow, and P. R Tingate, Fission track annealing in apatite: Track length measurements and the form of the Arrhenius plot, *Nucl. Tracks Radiat. Meas., 10*, 323-328, 1985.

Green, P. F., I. R. Duddy, A. J. W. Gleadow, P T. Tingate, and G. M Laslett, Thermal annealing of fission tracks in apatite, 1, A qualitative description, *Chem. Geol., 59*, 237-253, 1986.

Green, P. F., I. R Duddy, G M. Laslett, K. A Hegarty, A. J. W. Gleadow, and J. F. Lovering, Thermal annealing of fission tracks in apatite, 4, Quantitative modeling techniques and extension to geological time scales, *Chem. Geol , 79*, 155-182, 1989a.

Green, P. F , I R. Duddy, A. J. W. Gleadow, and J. F Lovering, Apatite fission track analysis as a paleotemperature indicator for hydrocarbon exploration, in *Thermal History of Sedimentary Basins*, edited by N D. Naeser and T. H. McCullogh, pp. 181-195, Springer-Verlag, New York, 1989b.

Hamilton, W. B., Detachment faulting in the Death Valley region, California and Nevada, *U.S. Geol. Surv Bull , B1790*, 51-85, 1988.

Hamilton, W. B., "Sevier Desert Detachment," Utah, A nonexistent structure, *Geol. Soc. Am Abstr. Programs, 26*, 57, 1994.

Hill, E. J., S. L. Baldwin, and G. S. Lister, Unroofing of active metamorphic core complexes in the D'Entrecasteaux Islands, Papua New Guinea, *Geology, 20*, 907-910, 1992.

Hintze, L. F., Geologic map of Utah, scale 1:500,000, *Utah Geol. Miner. Surv.*, Salt Lake City, 1980.

Hintze, L. F., Preliminary geologic map of the Marjum Pass and Swasey Peak SW quadrangles, Millard County, Utah, *Misc. Field Stud. Map, U.S. Geol. Surv., MF1332*, 1981.

Hintze, L F., Geologic history of Utah, *Brigham Young Univ. Geol. Stud., 7*, 202 pp., 1988.

Hintze, L. F., Interim geologic map of the Oak City North quadrangle, Utah and Millard counties, Utah, *Utah Geol. Surv. Open-File Rep., 221*, 1991a.

Hintze, L. F., Interim geologic map of the Oak City South quadrangle, Utah and Millard counties, Utah, *Utah Geol. Surv. Open-File Rep., 217*, 1991b.

Hintze, L. F., Interim geologic map of the Duggins Creek quadrangle, Millard County, Utah, *Utah Geol. Surv. Open-File Rep., 224*, 1991c.

Hintze, L. F., Interim geologic map of the Scipio Pass quadrangle, Millard County, Utah, *Utah Geol Surv. Open-File Rep., 222*, 1991d.

Hintze, L. F , Interim geologic map of the Fool Creek Peak quadrangle, Juab and Millard counties, Utah, *Utah Geol. Surv. Open-File Rep , 220*, 1991e.

Hintze, L. F., Interim geologic map of the Williams Peak quadrangle, Juab and Millard counties, Utah, *Utah Geol. Surv. Open-File Rep , 223*, 1991f

Holladay, J. C., Geology of the northern Canyon Range, Millard and Juab Counties, Utah, *Brigham Young Univ. Geol Stud., 31*, 1-28, 1984.

Hoover, J. D., Periodic Quaternary Volcanism in the Black Rock Desert, Utah, *Brigham Young Univ Geol Stud., 21*, 3-72, 1974.

Howard, K. A., and D. A. Foster, Thermal and unroofing history of a thick, tilted Basin-and-Range crustal section in the Tortilla Mountains, Arizona, *J. Geophy. Res., 101*, 511-522, 1996.

Hurford, A. J., and P F. Green, The zeta age calibration of fission track dating, *Chem. Geol., 1*, 285-317, 1983.

Ketcham, R. A., R. A., Donelick, J. K , Linn, and J D., Walker, Effects of kinetic variation on interpretation and modeling of apatite fission track data, application to central Utah, *Geol Soc. Am. Abstr. Programs, 28*, 441, 1996.

Ketcham R. A , W. D Carlson, and R. A. Donelick, Variability of apatite fission track kinetics, III, Extrapolation to geological time scales, *Am. Mineral., 84*, 1235-1255, 1999.

Laslett, G. M., W. S. Kendall, A. J. W. Gleadow, and I. R. Duddy, Bias in the measurements of fission track length distributions, *Nucl. Tracks Radiat. Meas., 6*, 79-85, 1982.

Laslett, G. M., P. F., Green, I. R., Duddy, and A. J. W. Gleadow, Thermal annealing of fission tracks in apatite, 2, A quantitative analysis, *Chem. Geol., 65*, 1-13, 1987.

Lawton, T F., D. A. Sprinkel, P. G. DeCelles, G Mitra, A. J Sussman, and M. P. Weiss, Stratigraphy and structure of the Sevier thrust belt and proximal foreland-basin system in central Utah; a transect from the Sevier Desert to the Wasatch Plateau, in *Mesozoic to Recent geology of Utah*, edited by P. K Link, *Brigham Young Univ. Geol. Stud., 42*, 33-67, 1997.

Lee, J., Rapid uplift and rotation of mylonitic rocks from beneath a detachment fault; insights from potassium feldspar $^{40}Ar/^{39}Ar$ thermochronology, northern Snake Range, Nevada, *Tectonics, 14*, 54-77, 1995.

Lee, J., E. L., Miller, and J. F. Sutter, Ductile strain and metamorphism in an extensional tectonic setting: A case study from the northern Snake Range, Nevada, U.S.A , in *Continental extensional tectonics*, edited by M. P. Coward et al , Geol. Soc. Spec Publ., *28*, 267-298, 1987

Lindsey, D. A., R K Glanzman, C. W. Naeser, and D J. Nichols, Upper Oligocene evaporites in basin fill of Sevier Desert region, western Utah, *AAPG Bull., 65*, 251-260, 1981.

Lindsey, D. A., Tertiary volcanic rocks and uranium in the Thomas Range and northern Drum Mountains, Juab County, Utah, *U.S. Geol Surv. Prof. Pap., P1221*, 71 pp., 1982.

Linn, J. K., Mesozoic and Cenozoic thermal history of the Canyon Range, Pavant Range, and vicinity, Central Utah Ph D thesis, Univ of Kans., Lawrence, 247 pp., 1998.

Lister, G. S , and G. A. Davis, The origin of metamorphic core complexes and detachment faults formed during Tertiary continental extension in the northern Colorado River region, U.S A., *J Struct. Geol , 11*, 65-94, 1989.

McDonald, R. E , Tertiary tectonics and sedimentary rocks along the transition: Basin and Range province to plateau and thrust belt province, Utah, *Rocky Mountain Assoc. of Geologists Symposium*, p. 281-317, 1976.

Millard, A. W., Structure and stratigraphy of the southern Canyon Range, Millard and Juab counties, Utah, *Geol. Soc. Am Abstr Programs, 15*, 379, 1983

Miller, E. L., P. B Gans, J. Lee, The Snake Range décollement, eastern Nevada, in *Cordilleran Sect. Geol. Soc. Am. Centennial Field Guide*, vol. 1, 77-82, 1983

Miller, E. L., T A. Dumitru, R. Brown, and P B. Gans, Rapid Miocene slip on the Snake Range-Deep Creek Range fault system, east-central Nevada, *Geol. Soc. Am. Bull., 111*, 886-905, 1999.

Mitchell, G. C., and R. E. McDonald, Subsurface Tertiary strata, origin, depositional model and hydrocarbon exploration potential of the Sevier Desert basin, west central Utah, *Utah Geol. Assoc. Publ., 16*, 533-556, 1987.

Mitra, G., and A. J. Sussman, Structural evolution of connecting splay duplexes and their implication for critical taper· An example based on geometry and kinematics of the Canyon Range culmination, Sevier Belt, central Utah, *J. Struct. Geol , 19*, 503-521, 1997

Mitra, G., N. Pequera, A. J. Sussman, and P G. DeCelles, Evolution of structures in the Canyon Range thrust sheet (Sevier fold-and-thrust belt) based on field relations and microstructural studies, *Geol. Soc. Am. Abstr. Programs, 26*, 527, 1994.

Morris, T. H., and G. F. Hebertson, Large-Rock avalanche deposits, eastern Basin and Range, Utah: Emplacement, diagenesis, and economic potential, *AAPG Bull., 80*, 1135-1149, 1996.

Naeser, C. W., The fading of fission tracks in the geologic environment-data from deep drill holes. *Nucl. Tracks Radiat. Meas., 5*, 248-250, 1981.

Otton, J K., Western frontal fault of the Canyon Range: Is it the breakaway zone of the Sevier Desert Detachment?, *Geology, 23*, 547-550, 1995.

Planke, S., and R B. Smith, Cenozoic extension and evolution of the Sevier Desert Basin, Utah, from seismic reflection, gravity, and well log data, *Tectonics, 10*, 345-365, 1991.

Price, D. E., Timing, magnitude, and three-dimensional structure of detachment-related extension, Mineral Mountains, Utah, M.S thesis, Univ. of Utah, Salt Lake City, 67 pp., 1998

Rietbrock, A , C. Tiberi, F. Scherbaum, and H. Lyon-Caen, Seismic slip on a low angle normal fault in the Gulf of Corinth; evidence from high-resolution cluster analysis of microearthquakes, *Geophy. Res. Lett., 23*, 1817-1820, 1996.

Rigo, A., H. Lyon-Caen, R. Armijo, A Deschamps, D. Hatzfeld, K. Makropoulos, P.

Papadimitriou, and I. Kassaras, A microseismic study in the western part of the Gulf of Corinth (Greece), implications for large-scale normal faulting mechanisms, *Geophys. J. Int*, *126*, 663-688, 1996.

Royse, F, Case of the phantom foredeep: Early Cretaceous in west-central Utah, *Geology*, *21*, 133-136, 1993.

Sorel, D., A Pleistocene and still-active detachment fault and the origin of the Corinth-Patras Rift, Greece, *Geology*, *28*, 83-86, 2000.

Stockli, D F, Regional timing and spatial distribution of Miocene extension in the northern Basin and Range Province, Ph.D. thesis, Stanford Univ., Stanford Calif., 239 pp., 1999

Stockli, D. F., K. A Farley, and T. A Dumitru, Calibration of the (U-Th)/He thermochronometer on an exhumed normal fault block in the White Mountains, eastern California and western Nevada, *Geology, 28*, 983–986, 2000.

Sussman, A. J., Geometry, deformation history, and kinematics in the footwall of the Canyon Range thrust, central Utah, M.S. thesis, Univ. of Rochester, Rochester, New York, 119 pp., 1995.

Swank, W. J, Structural history of the Canyon Range thrust, M.S. thesis, 46 pp., Ohio State Univ., Columbus, Ohio, 1978.

Villien, A., and R M Kligfield, Thrusting and synorogenic sedimentation in central Utah, in *Paleotectonics and Sedimentation* edited by J. A. Peterson, *AAPG Mem.*, *41*, 281-307, 1986.

Von Tish, D. B., R. W. Allmendinger, and J W. Sharp, History of Cenozoic extension in central Sevier Desert, west-central Utah, from COCORP seismic reflection data, *AAPG Bull*, *69*, 1077-1087, 1985.

Vrolijk, P, R A. Donelick, J. Queng, and M. Cloos, Testing models of fission track annealing in apatite in a simple thermal setting· Site 800, Leg 129, *Ocean Drill Program Results*, *129*, 169-176, 1992

Wagner, G, and P Van den haute, Fission track dating, 285 pp, Kluwer Acad Norwell, Mass., 1992

Walker, J. D., and J. M Bartley, New thrust fault relations in the Beaver Lake Mountains, southern Utah, and regional correlation of Sevier thrusts, *Geol. Soc. Am. Abstr. Programs*, *23*, 107, 1991.

Wernicke, B. P, Low-angle normal faults in the Basin and Range Province; nappe tectonics in an extending Orogen, *Nature*, *291*, 645-648, 1981.

Wernicke, B. P., Uniform-sense normal simple shear of the continental lithosphere, *Can. J. Earth Sci.*, *22*, 108-125, 1985.

Wernicke, B. P., Cenozoic extensional tectonics of the U S. Cordillera, in *The Cordilleran Orogen, Conterminous U.S.*, vol. G3, *Decade of North American Geology*, edited by B. C. Burchfiel et al., pp. 553-581, Geol. Soc. of Am., Boulder, Colorado, 1992.

Wernicke. B., and B. C. Burchfiel, Modes of extensional tectonics, *J Struct Geol.*, *4*, 105-115, 1982.

Wernicke, B. P., and G. J. Axen, On the role of isostasy in the evolution of normal fault systems, *Geology*, *16*, 848-851, 1988

Wills, S, and M. H. Anders, Western frontal fault of the Canyon Range, is it the breakaway zone of the Sevier Desert detachment?, Discussion, *Geology*, *24*, 667-669, 1996.

Wills, S., and M H Anders, Tertiary normal faulting in the Canyon Range, eastern Sevier Desert, *J. Geol*, *107*, 659-681, 1999

T. A. Dumitru, Department of Geological and Environmental Sciences, Stanford University, Stanford, CA 94305
(Dumitru@pangea.stanford.edu).

J K. Linn, Eagan McAllister Associates, Inc., P O. Box 986, Lexington Park, MD 20653 (Jon_Linn@emainc.com).

D. F. Stockli, Division of Geological and Planetary Sciences, California Institute of Technology, MS 100-23, Pasadena, CA 91125 (stockli@gps.caltech.edu)

J. D Walker, Department of Geology, University of Kansas, Lawrence, KS 66045 (jdwalker@ukans edu)

(Received May 23, 2000;
revised January 26, 2001;
accepted March 9, 2001.)